

On the Amphoteric Formalism and Electrolytic Reverse Complete Oxidation Processes in Relation to the Na-B-H-O System

Daniel L. Calabretta

*Centre de recherche en énergie, plasma et électrochimie,
Département de génie chimique et de biotechnologique, Université de Sherbrooke, Sherbrooke, Qc., Canada, J1K 2R1*

Available online 29 July 2013

Abstract

Solid light-alkaline-metal borohydride complete oxidation processes are the most akin to those currently used for vehicular propulsion. It is principally the lack of an efficient regeneration process that restricts the commercial use of these inorganic fuels. Within the framework of a so-called amphoteric formalism—an electrochemical reaction model—, among other matters, herein, water electrolysis, simple and complex electrolytic reverse hydrolysis, electrolytic reverse combustion, and, more generally, electrolytic reverse combustion oxidation processes are discussed.

Keywords: Electrolytic reverse complete oxidation; Hydrolysis; Hydrogen storage; Electrochemical reaction model; Concentration scale; Sodium borohydride

1. Introduction

Economic, pyrophoric, and toxic considerations aside, a vehicle's power-system is chosen based upon how far it can propel the vehicle on an equivalent charge and upon how long it takes to administer the charge; neglecting its balance-of-plant, a vehicular power-system is presumed to be comprised of at least one energy conversion devices and at least two reactants. For example, an electric vehicle's power-system may be comprised of a secondary battery and an electric motor, which are both energy conversion devices. But the secondary battery may be considered as a combination of an electrochemical cell—the electrodes and the electrolyte—and two reactants (e.g. elemental lithium and a transition metal oxide). As well, a vehicular hydrogen fuel cell (VHFC)—powered with the reactants molecular hydrogen (H_2) and ambient molecular oxygen (O_2)—in combination with an electric motor also constitutes a vehicular power-system. Of course the vehicular power-system of the masses is powered by the chemical reaction between hydrocarbons and ambient O_2 in internal combustion, diesel, or jet engines (i.e. energy conversion device) to overcome inertia and the frictional losses in the powertrain (i.e. transmission, driveshaft, differentials, etc.).

In recent years, through the implementation of regenerative braking, lithium ion battery, and nickel hydride battery technologies, vehicular power-systems have been trending towards electrification. In any case, the reasons for the O_2 -gasoline-internal combustion engine (ICE)-powertrain vehicular power-system's dominance over a fully electric one can be enumerated as follows: (i) one of the reactants, gasoline—a mixture comprised of the first and sixth lightest elements, is derived from the, thus far, naturally abundant substance, oil—, is a liquid with reasonable density that can be pumped and stored with relative ease; (ii) there is a negligible onboard weight penalty associated with the other reactant, O_2 , for it is taken directly from the ambient; and (iii) refueling takes minutes as opposed to hours.

Oil's scarcity can only increase with time; but, in order to reap the benefit of (ii), it seems critical to attempt to, as much as possible, replicate the status quo. In regards to (iii), a vehicle may be charged with H_2 in about the same amount of time it takes to charge a vehicle with a hydrocarbon fuel, but it seems implausible that the same will ever be said about any secondary battery, unless a discharged one is directly exchanged for a charged one.

In this article the author intends on articulating the reasons for why H₂ is an inherently inferior reactant to the family of vehicular hydrocarbons. Moreover, via the so-called amphoteric-formalism, the author's wish is to impress upon the reader the following arguments:

1. Light hydrocarbon complete oxidation processes are ones where carbon retains its positive character while, simultaneously, hydrogen's and O₂'s respective net negative and positive formal charges vanish.
2. Minus the noble elements (i.e. gases), elements and elemental molecules may be taken as symmetrical salts.
3. Only the onboard complete oxidation of certain *solid* light-alkaline-metal borohydrides can better the status-quo.

The three fundamental reasons for (3) are: (I) boron is the fifth lightest element that can have a maximum of three hydrogen atoms as nearest neighbours—all of which have negative formal charges; and (II) the complete oxidation of light-alkaline-metal borohydrides renders a solid metal oxide product that could potentially be regenerated off-board the vehicle. To the detriment of all vehicular hydrocarbon fuels, CO₂ is a gas at ambient conditions; hence, CO₂'s onboard capture and storage—for subsequent electrolytic, hydrocarbon regeneration—exceeds practical limits.

By reviewing state-of-the-art, onboard, H₂ storage technologies, the mode to onboard H₂ storage that can meet the United States Department of Energy's (USDoE) Ultimate energy capacity targets will firstly be identified. Then, the amphoteric formalism's reaction model rudiments in relation to the Na-B-O-H system will be expounded upon.

1.1 Onboard hydrogen storage

In 2003, the USDoE's Office of Energy Efficiency and Renewable Energy launched the FreedomCAR and Fuel Partnership Program. The program's focus was on identifying and solving the preeminent problems so that, by 2015, the original automotive equipment manufacturers would find it technically and economically feasible for 90% of the current, North American, light-duty vehicles to be substituted by H₂-powered analogues. This program's time-dependent target values serve as useful measures [1]. In comparison to the general target of ≥ 500 km charge⁻¹, the most obvious deficiency all of the prospective H₂-powered vehicles, thus far, has been their lack-luster driving ranges. The program's first report [2] identified onboard H₂ storage as being the most technically-challenging sub-program.

A H₂ storage material's toxicity, pyrophoricity, and cost are the foremost considerations; then, it is its energy capacities—both volumetric (kWh dm⁻³) and gravimetric (kWh kg⁻¹), with the former being the more crucial. Energy capacities are calculated by dividing the volume/mass of the maximum available, onboard H₂ energy—based on H₂'s lower heating value (LHV=33.3 kWh kg H₂⁻¹)—by the volume/mass of the H₂ storage material, its vessel, and its auxiliary components (i.e. balance of plant).

Because of: (a) the recent developments in vehicular hybridization; (b) the test results on actual as opposed to projected VHFC and H₂-powered, internal combustion engine (ICE) vehicle performance; and (iii) the original automotive equipment manufacturers' claims that vehicular architecture is now more accommodating towards H₂ storage systems, the ratios of the 2015 target volumetric and gravimetric energy capacities assigned in 2004 [3] and 2009 [4] are 2.08 and 1.67, respectively.. Along with the updated 2015 energy capacity targets (1.3 kWh dm⁻³ and 1.8 kWh kg⁻¹), a new (Ultimate) category—having ratios, as just defined, of 1.17 and 1.20, respectively—was suggested in the more recent report [1].

1.1.1 Molecular hydrogen storage

H₂'s type-1 [5] phase diagram [6] shows the material's narrow, low-temperature, liquid phase limits along with its low critical-point temperature (33 °K). The energy that is required to isothermally

compress a gas from its initial pressure (p_o) to its final pressure (p) can be estimated from, $\Delta G = RT \ln p/p_o$, where ΔG , R, and T denote the change in the system's free energy, the universal gas constant, and the absolute temperature. For onboard, compressed H₂ (CH2) storage systems rated to 35-70 MPa, an additional ~6 % should be included to account for irreversibilities; hence, if compared to H₂'s LHV, the useful work required to compress H₂ to the current, vehicular, upper value of 70 MPa is low (2.21 kWh kg⁻¹). However, as a H₂ pressure vessel's rating increases its gravimetric energy capacity must decrease, so it is impossible for CH2 systems to achieve the USDoE's desired energy capacity targets. Regardless, most of the H₂-powered vehicle testing [1] has been done with cylindrical, semi-spherical-capped vessels constructed of materials having high tensile strengths (ϵ). According to the relationship, $d_w/d_o = \Delta p / (2\epsilon - \Delta p) - d_o$, d_w , and Δp denoting the vessel's o.d., wall thickness, and pressure difference, respectively—a CH2 vessel's volumetric energy capacity increases to a point, and then decreases. Currently, vessel construction materials consist of carbon fiber and expensive polymers (e.g. Kevlar™). For vessels rated to 35 MPa, materials' costs [7] are in the order of 350 USD kg⁻¹ and increase quasi-exponentially with further pressurization [8].

The theoretical and actual energies [9] required for H₂'s liquefaction are 3.23 and 15.2 kWh kg H₂⁻¹. At 0.1 MPa, liquid H₂'s (LH2) density ($\rho_{LH2} = 0.078$ kg dm⁻³) is approximately one order of magnitude lower than that of gasoline's; therefore, the gasoline to LH2 volumetric energy capacity ratio is 3.8. As well, LH2 boil-off, which results from the ingress of heat through the cryogenic vessel's walls, is always significant. Notably, if compared to CH2 storage systems, the state-of-the-art, cryo-compressed LH2 ($\rho_{LH2} \leq 0.088$ kg dm⁻³) systems have significantly lower capital costs and meet the USDoE's revised, 2010 energy capacity targets [10].

1.1.2 Reversible metal hydrides

As certain light metal hydrides (e.g. LiH or LiBH₄) theoretically have higher energy capacities than either LH2 or CH2, in recent decades, 'reversible' metal hydrides have been widely considered as potential H₂ storage materials for transport applications. Metal hydride formations (i.e. $2M + xH_2 \rightarrow 2MH_x$) are usually exothermic processes that are often represented by type-2, pressure-composition phase diagrams [5] where composition—on the basis of atomic percentage—and the logarithm of pressure are the abscissa and ordinate, respectively. A metal hydride's dissociation pressure ($p_{H_2}^\circ$) is defined as the isothermal pressure at which a zero ΔG_{RXN}° is obtained. ΔH_{RXN}° and ΔS_{RXN}° are determined by plotting $\ln p_{H_2}^\circ$ against T^{-1} (i.e. van't Hoff diagram) after measuring $p_{H_2}^\circ$ at several temperatures. An authoritative report [11] was recently published on reversible metal hydride classifications, conventions, methodologies, and ambiguities in regards to the measurement of their thermodynamic properties. Problems such as low energy capacities, pyrophoricity, toxicity, high decomposition temperatures, and hysteresis have, thus far, prevented these materials from being employed as onboard H₂ storage materials. This mode to onboard H₂ storage also requires a heat exchange system for the removal and addition of heat to the metal hydride's bed during the exothermic H₂ release and endothermic H₂ uptake processes. Currently, only the light-metal (e.g. Li, B, Na, Mg, K, Al, and Ca) hydrides are being considered by the USDoE for onboard H₂ storage. Recent reviews on some of the more interesting metal hydrides are available [12, 13].

1.1.3 Off-board, regenerative metal hydrides

Recently, the USDoE defined ammonia borane (H₃NBH₃) and alane (AlH₃) as off-board, regenerative metal hydrides [14]. Like reversible metal hydrides, this mode of vehicular H₂ production occurs via the compounds' thermal decompositions; but, due to complex chemistry, the regenerative process must be done off-board. The USDoE's report [15] on the regeneration of H₃NBH₃ and AlH₃

*Corresponding author Tel.: +1 819 821 8000ext63238; fax: +1 819 821 7095

E-mail: danielcalabretta@gmail.com

indicates that straightforward processes do not currently exist. As well, these materials are pyrophoric and slowly decompose at ambient pressure.

1.1.4. Irreversible metal hydrides

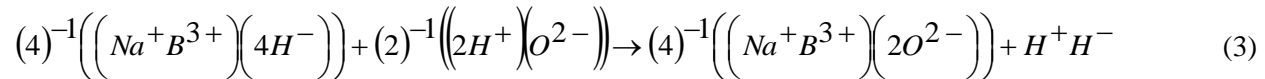
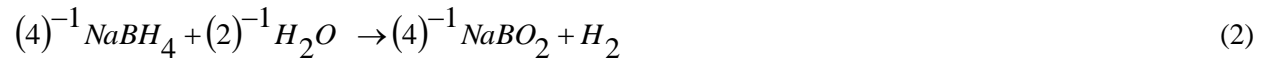
Between 2004 and 2007, if a metal hydride was being considered for the onboard production of H₂ via hydrolysis—defined here as the reaction between a metal hydride and water—, then the USDoE classified the metal hydride as being either *chemical* or *irreversible*. This mode to onboard H₂ storage assumes that the regeneration of the metal hydride (from its respective oxide species) takes place off-board the vehicle. Thus far, the vast majority of investigations of this mode of onboard H₂ storage have implicated the catalytic hydrolysis of caustic solutions containing several wt% sodium borohydride (NaBH₄) to an aqueous solution containing sodium metaborate (NaBO₂). A large number of investigations of this topic are available [16]. In 2007 the USDoE suspended its funding of aqueous NaBH₄/transportation fuel projects [17]. Neither the onboard H₂ generation [18, 19] nor the off-board NaBH₄ regeneration [20-25] processes satisfied the USDoE's targets (energy capacities, recycling efficiencies, costs, etc.). The two fundamental problems with this approach to onboard H₂ generation are: (i) NaBH₄ is diluted by a solvent (H₂O); and (ii) at least three onboard compartments (hydrolysis reactor, fuel, and waste) are required. Direct NaBH₄ fuel cell technologies [26, 27] suffer from the same shortcomings.

1.2 On the likeness of hydrocarbons and metal hydrides

Steam hydrocarbon reformation processes and metal hydride hydrolysis processes are analogous to one another; they are ones where, on an equivalent basis, M-H and H-O pairs rearrange themselves to form H-H and M-O pairs—where M, H, and O represent *atomic* metal, hydrogen, and oxygen, respectively. However, in contrast to steam hydrocarbon reformation processes, metal hydride hydrolysis processes result in solid oxide species at near-ambient conditions.

In essence, metathesis reactions—also known as double decomposition, reciprocal, or exchange reactions—involve two *ionic compounds*, where, upon their mixing, without there ever being any net change in any of the *elements'* oxidation states, there is a tendency towards the formation of stable pairs; hence, (Eq. 1) holds, where A and B are cations, C and D are anions, and q_A , q_B , etc. are their respective absolute charges. Now, if H₂ is substituted by H⁺H⁻, and if the hydrogen that are nearest neighbours to O (i.e. H₂O) and M are taken as H⁺ and H⁻, respectively, and if it is supposed that the oxygen and metal are ions that can be substituted by O²⁻ and M^{q+}, then this *general relationship* [28] applies itself to both the metal hydride hydrolysis and steam hydrocarbon reformation processes. In regards to NaBH₄ hydrolysis (Eq. 2), by substituting $H^+ = A$, $Na^+ + B^{3+} = X^{4+} = B$, $H^- = C$, and $O^{2-} = D$, from (Eq. 2) into (Eq. 1) we obtain (Eq. 3), which bears likeness to the overall steam methane reformation process (Eq. 4).

$$(q_C q_B)^{-1} B q_C C q_B + (q_A q_D)^{-1} A q_D D q_A \rightarrow (q_D q_B)^{-1} B q_D D q_B + (q_C q_A)^{-1} A q_C C q_A \quad (1)$$



Complete oxidation processes of either hydrocarbons—what is commonly referred to as combustion—or metal hydrides are simply the steam hydrocarbon reformation or metal hydride hydrolysis processes in combination with the water formation process. In either case, during complete oxidation, the

formal charge of hydrogen goes from being hydridic (H^-) to being protonic (H^+). Then it is debatable as to whether or not hydrocarbons, such as gasoline and diesel, would be more appropriately characterized as *carbon hydrides*. However, metal oxides are solids at near-ambient temperatures whereas CO_2 is a gas. The natural state of the former species gives rise to the possibility of achieving of simple metal oxide-to-metal hydride regeneration processes.

1.3 Onboard metal hydride complete oxidation processes

On a thermodynamic basis, the complete oxidation of some *solid*, light-alkaline-metal borohydrides ($\sum M^+, B^{3+}/H$) resembles the status quo. Several investigations of solid $NaBH_4$ hydrolysis reactors have recently been reported [29-33]. In order to surpass the present-day, vehicular fuel's volumetric and gravimetric energy capacities, these unconventional fuels' onboard complete oxidation processes are strictly limited. Fig. 1(a) shows the schematic of the crude flow diagram of the ideal, onboard, metal hydride complete oxidation process; the metal hydride's container is also its hydrolysis reactor and the H_2O required for its hydrolysis is supplied directly from the vehicular H_2 fuel cell (VHFC). The schematic of the crude flow diagram of a hybrid, onboard, chemical hydride, complete oxidation process is shown in Fig. 1(b). A small vessel of CH_2 , a condenser, and a H_2O storage vessel are incorporated into the ideal flow process; the most former's utility is three-fold: (i) it ensures the initiation of H_2O formation; (ii) it serves as a means to forcibly pump H_2O into the hydrolysis reactor; and (iii) it acts as an intermediate storage vessel for the H_2 produced via hydrolysis. Evidently, a VHFC based on solid oxygen anion electrolytes (SOAEs), as opposed to solid hydrogen cation electrolytes (SHCEs), is preferable for this mode of onboard H_2 storage.

Consider the 50mol%NaH- $NaBH_4$ (Na_2BH_5) mixture that was previously remarked upon [34]. By combining the ambient, facile hydrolysis of NaH (Eq. 6) with the exothermic process [35] at elevated temperature (Eq. 5), it is found that disodium oxide (Na_2O) is a catalyst for the hydrolysis of solid $NaBH_4$ (Eq. 2). Table 1 lists Na_2BH_5 's net energy capacities so that they can be compared with the USDoE's 2015 and Ultimate energy capacity targets [1]. The minimum and maximum amount of product mass/volume can be calculated under the assumptions that 100% conversion of the fuel's hydrolysis (Eq. 7) and complete oxidation (Eq. 9) processes. The USDoE's gravimetric energy capacity calculation for onboard hydrogen storage systems that gain weight during discharge includes the maximum possible weight of the system. *But this constraint should not be considered as being crucial for transport applications; rather, within reason, the fuel's initial volume and its respective oxide's density should be of paramount concern.* For this fuel mixture, in order to maintain the highest volumetric energy capacity possible while capturing the maximum amount of water for a subsequent electrolytic reverse complete oxidation (ERCO) process, the ratio $n_{H_2O}/n_{Na_4B_2O_5}$ should not exceed a value of ~ 1.3 . Beyond the USDoE's Ultimate target, the volumetric energy capacity of pure Na_2BH_5 leaves 1.35 times the volume required for the fuel available for the volume of the hydrolysis reactor and its auxiliary components. Any reversible metal hydride (1.1.2) could also be considered as a chemical/irreversible metal hydride (1.1.3) and their net gravimetric energy capacities double if they are contemplated in this way, and the same routine as the one used to obtain the values in Table 1 can be applied.

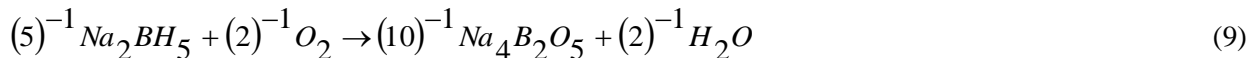
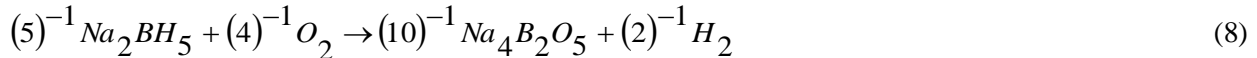
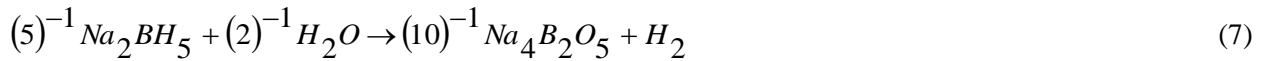
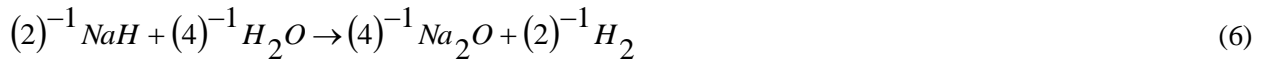
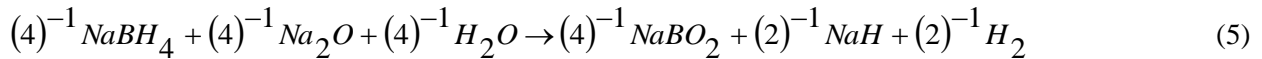


Table 1 Calculated net energy capacities of pure and variably hydrolyzed Na_2BH_5

| Energy capacity | Na_2BH_5 | $\text{Na}_4\text{B}_2\text{O}_5$ | $\text{Na}_4\text{B}_2\text{O}_5 \cdot 2\text{H}_2\text{O}$ | $\text{Na}_4\text{B}_2\text{O}_5 \cdot 5\text{H}_2\text{O}$ |
|---------------------------------|--------------------------|-----------------------------------|---|---|
| $\text{kg H}_2 \text{ kg}^{-1}$ | 16.3% | 10.4% | 8.8% | 7.1% |
| kWh kg^{-1} | 5.4 | 3.5 | 2.9 | 2.4 |
| $\text{kg H}_2 \text{ dm}^{-3}$ | 0.16 | 0.26 | 0.13 | 0.09 |
| kWh dm^{-3} | 5.4 | 8.5 | 4.3 | 2.9 |

*net energy capacities have been calculated using the literature value densities for NaH [51] (0.92 kg dm^{-3}), NaBH_4 [51] (1.07 kg dm^{-3}), $\text{Na}_4\text{B}_2\text{O}_5$ [52] (2.46 kg dm^{-3}), and H_2O (1.00 kg dm^{-3})

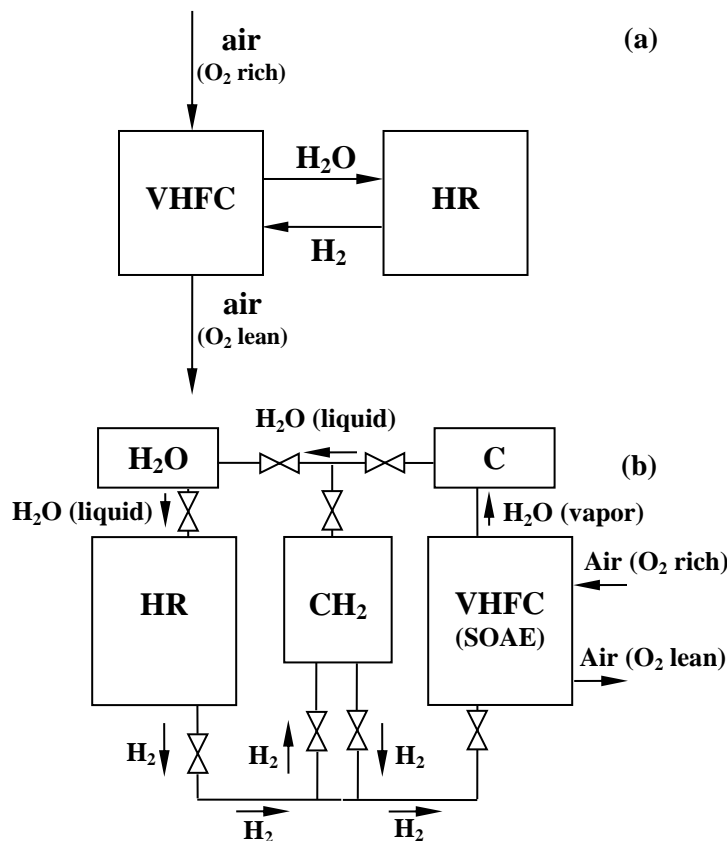


Fig. 1 Schematics of the crude flow diagram of the (a) ideal and (b) hybrid onboard, chemical hydride, complete oxidation processes—hydrolysis reactor (HR); vehicular H_2 fuel cell (VHFC); pressurized H_2 storage vessel (CH2); H_2O condenser (C) and storage (H_2O)

1.4 Electrolytic reverse complete oxidation processes

A simple electrolytic process for the regeneration of metal hydrides from their respective oxides is not readily available. Elucidation of such a method and attempts to perform proof-of-concept thereon has been the author's principal preoccupation for several years. Previously, the relevant $\text{Na}^+, \text{B}^{3+}/\text{H}^+, \text{O}^{2-}$ liquidus topology was experimentally determined and, among other matters, a simple electrolytic process for the regeneration of Na_2BH_5 from sodium pyroborate ($\text{Na}_4\text{B}_2\text{O}_5$) was proposed [34]. The electrolysis unit operations that were given in the journal article and thesis [36] have been more clearly defined as electrolytic reverse combustion (ERC) and electrolytic reverse hydrolysis (ERH), respectively. A patent was recently awarded for the latter type [37]. In a recent proceedings publication [38], the author

*Corresponding author Tel.: +1 819 821 8000ext63238; fax: +1 819 821 7095

E-mail: danielcalabretta@gmail.com

introduced some of the rudiments of a so-called amphoteric formalism—an electrochemical reaction model.

The simplest embodiments of the hypothetical processes for the electrolytic regeneration of Na_2BH_5 from $\text{Na}_4\text{B}_2\text{O}_5$ are represented by the schematics shown in Fig. 2(a) (ERH) and Fig. 2(b) (ERC); they are the reverse of the processes given by (Eq. 7) and (Eq. 8), respectively; they are exceedingly simple and can be described by the following: (A) the cathode is in contact with a solution of metal oxides with their respective hydrides and dissolved H_2 and the most latter most species is electro-reduced to hydride ions (H^-) which invokes the reduction of the metal oxide species to oxygen anions (O^{2-}) and its metal hydride species; (B) a dense SOAE facilitates the transport of O^{2-} in the internal circuit and negates *molecular* cross-over between the electrolytic cell's two distinct compartments so that the back-reaction is avoided; and (C) either H_2O vapour (ERH) or O_2 gas (ERC) formation occurs at the anode.

It has, of course, been tacitly assumed that neither the SOAE nor the electrodes are reactive or significantly soluble with or in the electrolytic cell's anolyte and catholyte. While the catholyte mixtures may be deemed as unusual by many, these mixtures are interesting in both the practical and fundamental sense. The previous article [34] articulates the reasons why only the liquid, anhydrous, metal oxide/hydride catholytes could be considered for these electrolytic processes.

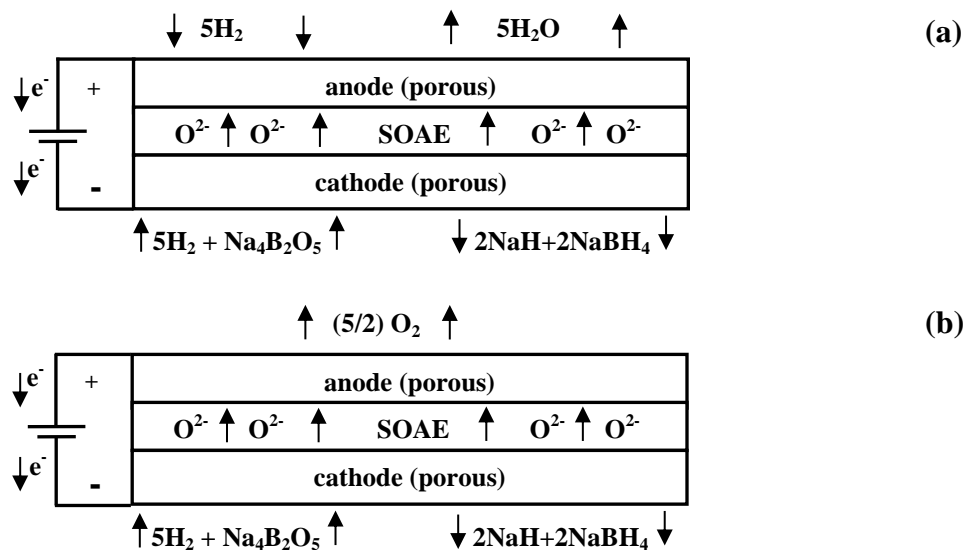


Fig. 2 (a) Schematic of an ERH cell illustrating the production of H_2O and Na_2BH_5 from H_2 and $\text{Na}_4\text{B}_2\text{O}_5$; (b) Schematic of an ERC cell illustrating the production of O_2 and Na_2BH_5 from H_2 and $\text{Na}_4\text{B}_2\text{O}_5$

As they relate themselves to the regeneration of Na_2BH_5 from $\text{Na}_4\text{B}_2\text{O}_5$, the schematics illustrating the crude flow diagrams for the hypothetical, ERCO processes incorporating the ERH and ERC unit operations are given in Fig. 3. Ostensibly, the water electrolysis (WE) and dehydration (D) unit operations do not pose as technological barriers in the overall development of these processes. However, at the time of this writing, the ERH and ERC unit operations have remained hypothetical.

Now, onboard hydrolysis and the off-board ERCO processes implicate solid, molten salt, aqueous, gaseous, and metallic media. The amphoteric formalism, in many respects, may be viewed as an attempt to unify historically different concentration scales; it assumes that, with the exception of the noble gasses, any mixture of any media, including elemental molecules and the like, may be treated as being comprised entirely of ions. This article's principal aim is to bring forth the formalism's reaction model rudiments—particularly as they concern electrochemical processes. In a future article the formalism's solution model rudiments will be presented.

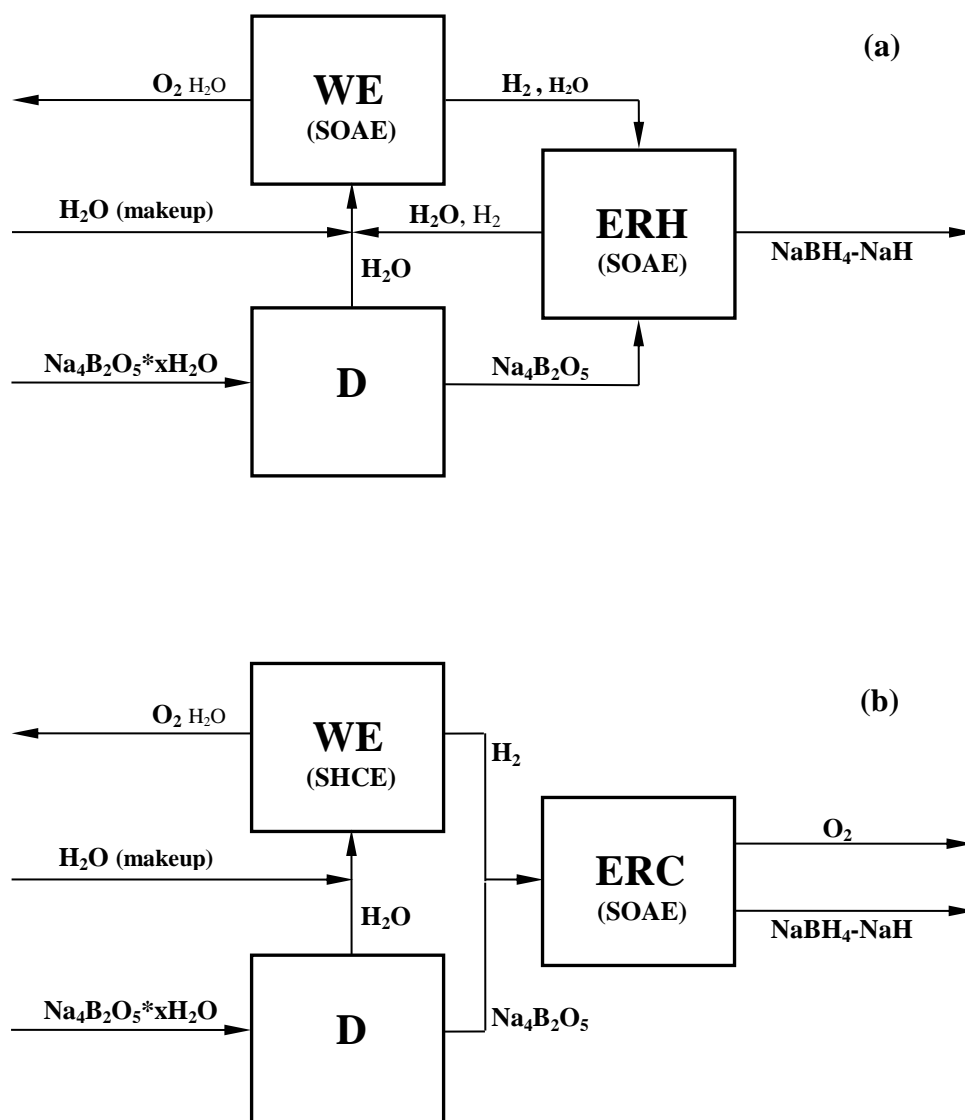


Fig. 3 Block diagrams for steady-state ERCO processes (~ 1.0 MPa; ~ 823 °K)—(a) ERH-based process; (b) ERC-based process—D - dehydration; WE - water electrolysis

2. On the amphoteric formalism's electrochemical reaction model rudiments

Chemical thermodynamics' concentration scales are arbitrary; the pH, molecular/atomic/mole/mass ratios, molecular/atomic/mole/mass fractions, partial pressures, ionic fractions, equivalent ionic fractions, pair fractions, among others [39-41] have had varying degrees of utility for the graphical representation of macroscopic mixtures. A universal concentration system, however, does not exist [39].

For the specification of ionic species in a mixture at equilibrium, in his initial theoretical discussion of the perfect electro-chemical apparatus, Gibbs [42] used densities (mass of solutum per unit volume of solution). Guggenheim's preferred concentration scale for ionic species was given by the dimensionless unit of molality [53], m_i —equivalent to the ratio, r_i/r° , where r° is the reference state of one mole of the ionic species per kilogram of solvent—, and expressed the absolute potential of an ionic species, μ_i , as $RT \ln a_i$, where, $a_i = \lambda^\circ m_i \gamma_i$, with λ° and γ_i being taken as a solvent dependent coefficient and the ionic species' activity coefficient, respectively. Under this formalism, $\gamma_i \rightarrow 1$ as $m_i \rightarrow 0$. A dimensionless concentration unit, like the mole fraction, must be used in the logarithmic terms or else the term $RT \ln a_i$ will not have the units of energy. It is worth mentioning that only the ionic fraction, equivalent ionic fraction, molality, and pH scales implicate ionic species.

In his discussion pertaining to the concept of molecular resonance, L. Pauling [44] estimates that ~5% of H_2 's (molecular) bond-energy can be attributed to the ionic structures H^+H^- and HH^+ , and following the discovery of liquid lithium hydride's high ionic conductivity, in his seminal paper [44], G. N. Lewis suggested that *atomic* hydrogen should be positioned upon the periodic table's IA and VIIA columns. The general reciprocal relationship (Eq. 4) shows that, by convenience, one may treat H_2O and H_2 as salts.

In using conventional notation, at a specified temperature and pressure, the Gibbs energy of reaction for H_2O formation (${}^{OH}\Delta G$) is given by (Eq. 10) where the activity of the product water (a_{H_2O}) and the fugacities of the gaseous reactants (f_{H_2}, f_{O_2}) define the system's composition, the standard Gibbs energy of water formation (ΔG°) is defined as the chemical energy when H_2O , H_2 , and O_2 are all in their standard states (Eq. 11), and the equilibrium concentrations are calculated from the equilibrium constant (K_{eq}) when ${}^{OH}\Delta G$ is null (Eq. 12).

There are two points of contention that must be recognized: (i) it does not seem plausible that one can have a three component system where all three components simultaneously have unit activity/fugacity; rather, only in a unary system is it possible for an independently variable component to have unit activity; and (ii), there are an infinite number of values that can be assigned to the activity and fugacities so that (Eq.12) is satisfied.

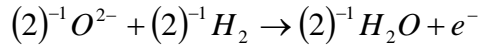
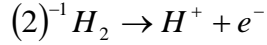
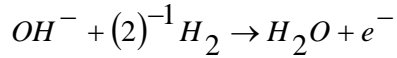
$$\Delta G_{rxn} = \Delta G^\circ_{rxn} + RT \ln \left(\frac{a_{H_2O}^2}{f_{H_2}^2 f_{O_2}} \right) \quad (10)$$

$$\Delta G_{rxn} = \Delta G^\circ_{rxn} + RT \ln \left(\frac{1}{1^2 1} \right) = \Delta G^\circ_{rxn} \quad (11)$$

$$\exp \left(\frac{-\Delta G^\circ_{rxn}}{RT} \right) = K_{eq} = \frac{a_{H_2O}^{\circ 2}}{P_{H_2}^{\circ 2} P_{O_2}^{\circ}} \quad (12)$$

The Nernst equation ($\Delta G = -nF\Delta E$) equates electrical energy to chemical energy. In classical electrochemical theory, for galvanic water formation, depending on if the electrolyte's makeup is deemed to be *basic* (Eq. 13), *acidic* (Eq. 14), or vapour/gas (Eq. 15) in character, three distinct half-reaction sets are used to define the process. These galvanic cells may be constructed via the use of liquid hydroxide anion electrolytes, SHCE (i.e. polymer electrolyte membrane), or SOAE, respectively. The latter two cells are illustrated in Table 2.

*Corresponding author Tel.: +1 819 821 8000ext63238; fax: +1 819 821 7095
E-mail: danielcalabretta@gmail.com



In aqueous electrochemistry, the hydrogen electrode potential, E , is expressed by (Eq. 16); its standard potential, E° , has been chosen by others to have a value of zero with respect to all other standard electrode potentials. The electrode potential is, however, undefined, for the proton's activity ($a_{H^{+}}$) would have to be assigned a value of unity, which implies that a monoprotic species is dissolved in water to a concentration of 1 mol L⁻¹. But it is unclear which specific anion(s) counterbalance the protons' charge. Furthermore, H₂ (gas) must continuously flow over a platinized platinum electrode; hence, an infinite reservoir of H₂ gas must be connected to the electrode in order to maintain a constant potential indefinitely—a situation that may be interpreted as one where H₂ constitutes the composition at the immediate vicinity of the electrode and the adjacent aqueous system constitutes the electrolyte. It is generally accepted that the pH scale is a notional one [45] that is severely limited in its temperature range.

$$E = E^{\circ} - \frac{RT}{2F} \ln \left(\frac{f_{H_2}}{a_{H^{+}}} \right) \quad (16)$$

Because of the ambiguity of the standard hydrogen electrode along with the lack of a universal, electrochemical concentration scale that is ambivalent to the type of medium (i.e. solid, gas, molten salt, aqueous, etc.) an alternate framework may be proposed. The forthcoming formalism avoids any differentiation between the solute and the solvent by viewing both the anolyte and catholyte as purely ionic mixtures. (This gross oversimplification's utility will become apparent.) Thus, the convention employed here is one where the pure, obvious compounds, such as H₂, NaH, H₂O, etc., both of the ionic concentrations are unity and so is their corresponding activity coefficients (γ_i s).

Then, without any farther limitations, it is assumed here that ionic bonding exists for all compounds and elements in their pure and most stable phase(s) at a given temperature and pressure; henceforth, the light elements H, B, O, Li, and Na will be regarded as the ionic mixtures H⁺H⁻, B³⁺B³⁻, O²⁺O²⁻, Li⁺Li⁻, and Na⁺Na⁻, respectively. Therefore, with the exception of the noble gases, this formalism extends the charge neutrality principle (Eq. 17) to all matter, where n_i and n_j , are the moles of the so-considered cations and anions, respectively, and q_i and q_j are the ions' absolute charges. The concentration unit that will be used throughout this discussion are defined herein as elemental equivalent ionic fractions (EEIF) (Eq. 18), which are akin to the equivalent ionic fractions that have been used by molten salt chemists for over a half-century [40].

$$\sum_i q_i n_i = \sum_j q_j n_j \quad (17)$$

$$Y_i = \frac{q_i n_i}{\sum_i q_i n_i}, \quad Y_j = \frac{q_j n_j}{\sum_j q_j n_j} \quad (18)$$

The phase rule, as it was initially derived [42], implicates independently variable components. Obviously ions cannot be treated as such. While the number of independently variable components has historically been taken to be equal to the number of ions minus one, as will be discussed shortly, under this formalism, additional relationships can be put into place to ensure that the number of composition variables that need to be specified is the same regardless of whether or not chemical species are viewed as being either ionic or covalent

2.1 Isothermal, isobaric, equivalent, elemental binary composition lines

Two types of elemental binary composition lines will be considered here: those where one obvious compound exists and those where no obvious compound exists. As general examples, the former and latter types will pertain to the H-O system (Fig. 4) and the Na-B system (Fig. 5), respectively. Composition lines are shown using both the (a) atomic fraction and (b) EEIF concentration scales. To be clear, obvious compounds are defined as those that are comprised of elements having definite formal charges or oxidation states so that in the extreme they may be considered as being ionic.

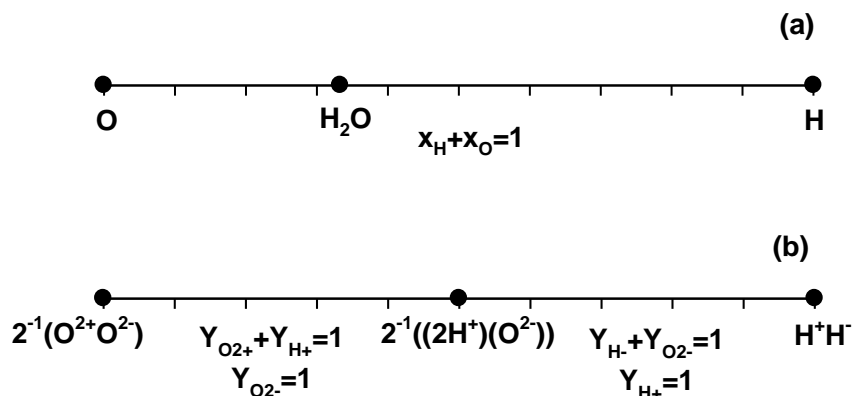


Fig. 4 Isothermal, isobaric, equivalent, elemental, H-O binary composition line shown on the basis of (a) molar atomic fractions and (b) EEIFs

At near-ambient temperatures and pressures, due to the spontaneous formation of H₂O—a compound where unambiguously hydrogen and oxygen have positive and negative formal charges, respectively—, H₂ and O₂ are unstable together. Here, two hydrogen cations (i.e. protons; H⁺) and one oxygen anion (O²⁻) constitute the water molecule, so that half of a mole of H₂O is equal to its equivalent quantity. (i.e. one mole of anionic charge counterbalanced by mole of cationic charge.) Mixtures of H₂-H₂O and O₂-H₂O are taken as the common-ion, sub-binary mixtures H⁺/H₂O²⁻ and O²⁻,H⁺/O²⁻, respectively. Then, on an equivalent basis (Eq. 19), while assuming that H₂ and O₂ are symmetric salts, and that H₂O is an asymmetric salt, it is found that the water formation process is one where half of a mole of H⁺ reduces one quarter of mole of oxygen cations (i.e. O²⁺) (Eq. 21), and by cancellation of the unaffected species we have the general expression (Eq. 22). Furthermore, if the hydroxide ion (OH⁻) is substituted by O²⁻ and H⁺ (i.e. O²⁻ + H⁺ = OH), then the aforementioned galvanic water formation half-reactions may be expressed by (Eq. 22) and (Eq. 23), and the electrode potentials for each amphoteric half-reactions may be expressed by (Eq. 24) and (Eq. 25).

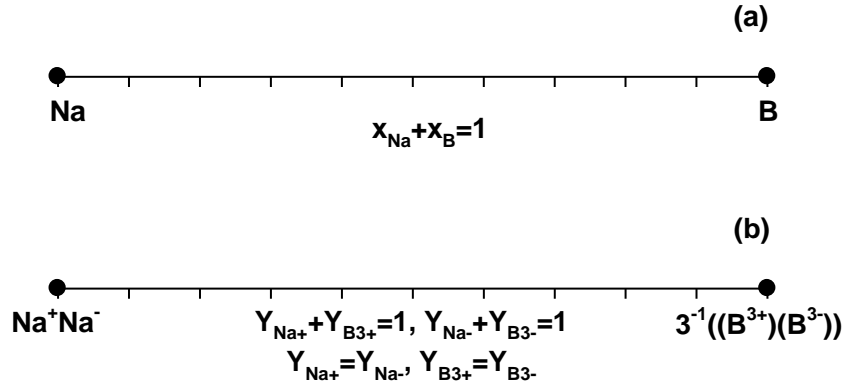
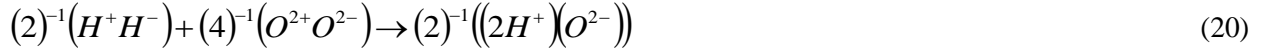


Fig. 5 Isothermal, isobaric, equivalent, elemental Na-B binary composition line shown on the basis of (a) molar atomic fractions and (b) EEIFs



$$H_E = H_{E^\circ} - (F)^{-1} RT \ln \left(\frac{a_{H^-}^{1/2}}{a_{H^+}^{1/2}} \right)$$

$$= H_{E^\circ} - ZT \ln \left(\frac{Y_{H^-}^{1/2} \gamma_{H^-}^{1/2}}{Y_{H^+}^{1/2} \gamma_{H^+}^{1/2}} \right) = H_{E^\circ} - ZT \left(\ln \left(\frac{Y_{H^-}^{1/2}}{Y_{H^+}^{1/2}} \right) + C \right) \quad (24)$$

$$O_E = O_{E^\circ} - (F)^{-1} RT \ln \left(\frac{a_{O^{2-}}^{1/4}}{a_{O^{2+}}^{1/4}} \right)$$

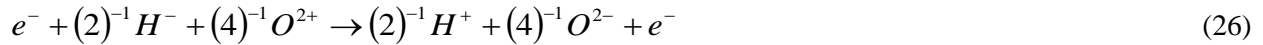
$$= O_{E^\circ} - ZT \ln \left(\frac{Y_{O^{2-}}^{1/4} \gamma_{O^{2-}}^{1/4}}{Y_{O^{2+}}^{1/4} \gamma_{O^{2+}}^{1/4}} \right) = O_{E^\circ} - ZT \left(\ln \left(\frac{Y_{O^{2-}}^{1/4}}{Y_{O^{2+}}^{1/4}} \right) + C \right) \quad (25)$$

For the standard electrode potentials ($^H E^\circ$, $^O E^\circ$, etc.) under consideration, when the temperature and pressure are specified, there can only be a hierarchy between them. Individually, they are assigned zero values at all temperatures and pressures. This has no physical significance as only potential differences between two electrode contacts can be measured, and is akin to Hess's law which states that, at STP, the elements' (and elemental molecules') absolute enthalpies are equal to zero and that the

compounds' absolute enthalpies are equal to the enthalpy of compound formation (ΔH_{RXN}°). The absolute entropies of all substances in their most stable state approach zero as the temperature approaches absolute zero. Unlike standard electrode potentials, electrode potential differences have physical meaning because their magnitudes can, in many instances, be measured by assembling a well-defined galvanic cell.

The water formation galvanic cells shown in Table 2 are representations of what the author deems to be perfect electrochemical cells. They are those that: (i) have anode and cathode compartments that can be treated as two independent systems where only the mixtures of independently variable components contained in each compartment/system is of interest; (the compositions of the individual phases of a multi-phase system are not of concern for now); (ii) the anolyte and catholyte are isolated from each other by an appropriate solid ion electrolyte where the transport numbers of the respective ions are unity; (iii) the electrodes and their contact material (with the external circuit) are made of the same material; (iv) the electrodes are porous and in physical contact with a dense solid ion electrolyte so that the amphoteric half-reactions occur at the triple boundary layer; (v) the electrodes are assumed to be completely inert and insoluble with the chemical species that constitute the anolyte and catholyte; and (vi) the material(s) that separate the anolyte and catholyte mixtures from the surroundings are inert, rigid bodies.

As is the case for all galvanic cells, the potential difference is measured while applying an infinite resistance between the electrodes' contacts so that an infinitesimal electronic current flows between them. Under such an arrangement, the anolyte and catholyte contained in their respective compartments are in dynamic equilibrium; hence, no appreciable net reaction(s) take place in either compartment. Then, from the logical combination of the two amphoteric half-reactions, the most general expression for electrochemical water formation is given by (Eq. 26). The electrochemical potentials (Eq. 27) of the charged species $\bar{\mu}_{e^-}^{-Cu}$, $\bar{\mu}_{H^-}$, etc. are expressed with the classical notation [43].



$$\bar{\mu}_{e^-}^{-Cu} + (4)^{-1} \bar{\mu}_{O^{2+}} + (2)^{-1} \bar{\mu}_{H^-} = (4)^{-1} \bar{\mu}_{O^{2-}} - (2)^{-1} \bar{\mu}_{H^+} + \bar{\mu}_{e^-}^{-Cu'} \quad (27)$$

$$\bar{\mu}_{e^-}^{-Cu} = \mu_{e^-}^\circ - F\phi^{Cu}$$

$$(2)^{-1} \bar{\mu}_{H^-} = (2)^{-1} \mu_{H^-}^\circ + RT \ln a_{H^-}^{1/2} - F\phi^S$$

$$(4)^{-1} \bar{\mu}_{O^{2+}} = (4)^{-1} \mu_{O^{2+}}^\circ + RT \ln a_{O^{2+}}^{1/4} + F\phi^S$$

$$(4)^{-1} \bar{\mu}_{O^{2-}} = (4)^{-1} \mu_{O^{2-}}^\circ + RT \ln a_{O^{2-}}^{1/4} - F\phi^S$$

$$\bar{\mu}_{e^-}^{-Cu'} = \mu_{e^-}^\circ - F\phi^{Cu'}$$

Substitution into (Eq. 27) renders (Eq. 28)

$$\begin{aligned} {}^{OH}(\phi^{Cu} - \phi^{Cu'}) &= {}^{OH}\Delta E = F^{-1}(-{}^{OH}\Delta G^{eq}) \\ &= -F^{-1}\left((4)^{-1} \mu_{O^{2-}}^\circ + (2)^{-1} \mu_{H^+}^\circ - (4)^{-1} \mu_{O^{2+}}^\circ - (2)^{-1} \mu_{H^-}^\circ\right) - F^{-1}RT \ln \left(\frac{a_{H^+}^{1/2} a_{O^{2-}}^{1/4}}{a_{H^-}^{1/2} a_{O^{2+}}^{1/4}}\right) \end{aligned} \quad (28)$$

Upon further substitution of $a_i = \gamma_i Y_i$ for the individual ions and

$$\begin{aligned} {}^{OH}\Delta E^\circ(T, P) &= -F^{-1}\left((4)^{-1} \mu_{O^{2-}}^\circ + (2)^{-1} \mu_{H^+}^\circ - (4)^{-1} \mu_{O^{2+}}^\circ - (2)^{-1} \mu_{H^-}^\circ\right) \\ &= -F^{-1}\left((2)^{-1} \mu_{H_2}^\circ + (4)^{-1} \mu_{O_2}^\circ - (2)^{-1} \mu_{H_2O}^\circ\right) = F^{-1}(-{}^{OH}\Delta G^{eq}(T, P)) \end{aligned}$$

*Corresponding author Tel.: +1 819 821 8000ext63238; fax: +1 819 821 7095

E-mail: danielcalabretta@gmail.com

we obtain (Eq. 29) and (Eq. 30), which are henceforth referred to as a modified Nernst equation (MNE). When temperature and pressure are specified the standard electrode potential difference, ${}^{OH}\Delta E^\circ$, is calculable from the independently variable components' absolute thermodynamic properties that may be determined from calorimetric measurements.

$$= {}^{OH}\Delta E^\circ - F^{-1}RT \left(\ln \left(\frac{Y_{H^+}^{1/2} \gamma_{H^+}^{1/2}}{Y_{H^-}^{1/2} \gamma_{H^-}^{1/2}} \right)^{H^+/H^-, O^{2-}} + \ln \left(\frac{Y_{O^{2-}}^{1/4} \gamma_{O^{2-}}^{1/4}}{Y_{O^{2+}}^{1/4} \gamma_{O^{2+}}^{1/4}} \right)^{O^{2-}/O^{2+}, H^+} \right) \quad (29)$$

$$= {}^{OH}\Delta E^\circ - ZT \left(\ln \left(\frac{Y_{H^+}^{1/2}}{Y_{H^-}^{1/2}} \right)^{H^+/H^-, O^{2-}} + \ln \left(\frac{Y_{O^{2-}}^{1/4}}{Y_{O^{2+}}^{1/4}} \right)^{O^{2-}/O^{2+}, H^+} + C \right) \quad (30)$$

If the electrochemical cell's compartments contain only components that are present on the H-O binary system (Fig. 4), then Y_{H^+} and $Y_{O^{2-}}$ are both equal to unity and the MNE is simplified further (Eq. 31).

$${}^{OH}\Delta E = {}^{OH}\Delta E^\circ + ZT \left(\ln \left(Y_{H^-}^{1/2} \right)^{H^+/H^-, O^{2-}} + \ln \left(Y_{O^{2+}}^{1/4} \right)^{O^{2-}/O^{2+}, H^+} + C \right) \quad (31)$$

Electrochemical heat of mixing studies experimentally determine the activity coefficients (γ_i), and could be performed on either the $H^+/H, O^{2-}$ or the $O^{2-}/O^{2+}, H^+$ common-ion, sub-binary system by employing either a SOAE or a SHCE, respectively, where the amphoteric half-reactions implicate the electro-active ions (i.e. the system's amphoteric element), and the non-electro-active ion is transported in the internal circuit. As a mixture's composition approaches that of either non-noble elements, elemental molecules, or obvious compounds its corresponding activity coefficients approach unity. For all other compositions, the activity coefficients are dependent on which solution model the modeller wishes to use. All thermodynamic solution models are concentration-scale dependent, but this is not the central theme of this article. To obtain a better idea of the possible solution models that are currently available, the reader is directed to the conformal ionic solution model [46] and the phenomenological modified quasi-chemical model [41]. For now, the logarithmic terms carrying all the activity coefficients are lumped together (C) in the MNE.

To summarize: (a) an elemental binary composition line having a single obvious binary compound may be divided at its midpoint into two common-ion, sub-binary composition lines; (b) for the perfect electrochemical cells considered here for obvious compound formation, only the half-reaction that implicates the amphoteric element is possible and the non-amphoteric species carries the internal current; (c) the material composition of either compartment is defined by the ratio of the amphoteric element's two EEIFs; (d) the reference composition for a compartment is defined as the molecule of an element, which is treated as a symmetrical salt; and (e) the potential for compound formation or mixing is expressed on an equivalent basis via the MNE.

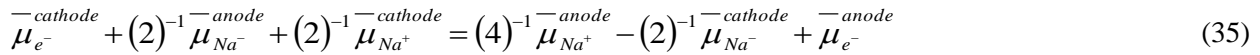
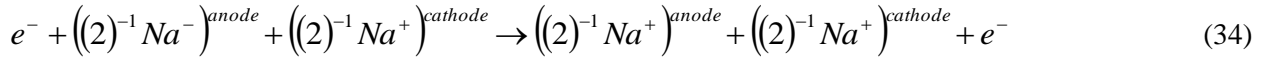
This formalism will now be extended to elemental binary systems for which no obvious compounds form and therefore cannot be divided into two common-ion, sub-binary composition lines (Fig. 5). The Na-B binary system, which has not been thoroughly studied [47], will be used as an example, and is classified as a non-common-ion elemental binary system.

In order for the elemental binary system to be defined by a single EEIF, along with the equations of charge neutrality ($Y_{Na^+} + Y_{B^{3+}} = 1$ and $Y_{Na^-} + Y_{B^{3-}} = 1$), it must be assumed that the EEIFs of the amphoteric elements' ions are present in equivalent amounts (i.e. $Y_{Na^+} = Y_{Na^-}$ and $Y_{B^{3+}} = Y_{B^{3-}}$).

Furthermore, for any galvanic cell that is constructed to measure the potential difference between two independent compartments of different compositions, only one of the two half-reactions, given by (Eq. 32) or (Eq. 33), can occur in both the anode and cathode compartments. Which particular amphoteric half-reaction is solely dependent on the type of solid ion electrolyte used in the construction of the cells. However, of the four ions, only the solid sodium cation electrolyte (SSCE) is known to exist (i.e. B^{3-} - Al_2O_3), but if there were to be solid ion electrolytes having pure conductance for the ions Na^+ , B^{3+} , or B^{3-} , the same analysis as what follows could also be applied.



For example, if a SSCE is considered for concentration cell, as one equivalent of electrons passes in the external circuit of a galvanic cell, one equivalent of Na^- is oxidized to Na^+ at the anode, two equivalents of Na^+ traverses the SSCE, and one equivalent of Na^+ is reduced to Na^- at the cathode. Evidently, at the cathode, an equivalent of B^{3+} would not be reduced to B^{3-} as this would indicate that formation of an obvious compound. Under these circumstances the electrochemical processes are expressed by (Eq. 34) and (Eq. 35), and the MNE is given by (Eq. 36).



$$\begin{aligned} {}^{NaB}(\phi^{Cu} - \phi^{Cu'})^{SSCE} &= {}^{NaB}\Delta E = F^{-1} \left(-{}^{NaB}\Delta G^{eq} \right) \\ &= -F^{-1} \left(2^{-1} \mu_{Na^-}^\circ + (2)^{-1} \mu_{Na^+}^\circ - (2)^{-1} \mu_{Na^+}^\circ - (2)^{-1} \mu_{Na^-}^\circ \right) - ZT \left(\ln \left(\frac{a_{Na^+}^{1/2}}{a_{Na^-}^{1/2}} \right)^{anode} + \ln \left(\frac{a_{Na^-}^{1/2}}{a_{Na^+}^{1/2}} \right)^{cathode} \right) \\ &= -ZT \left(\ln \left(\frac{a_{Na^+}^{1/2}}{a_{Na^-}^{1/2}} \right)^{anode} + \ln \left(\frac{a_{Na^-}^{1/2}}{a_{Na^+}^{1/2}} \right)^{cathode} \right) \\ &= -ZT \left(\ln \left(\frac{Y_{Na^+}^{1/2}}{Y_{Na^-}^{1/2}} \right)^{anode} + \ln \left(\frac{Y_{Na^-}^{1/2}}{Y_{Na^+}^{1/2}} \right)^{cathode} + C \right) = -ZTC \quad (36) \end{aligned}$$

The ratios of the EEIFs for both compartments are unity and this renders zero values for their logarithmic terms. C is a function of the temperature, pressure, and compositions in both compartments and its value may be determined experimentally. Evidently, when the two compartments are of identical composition, ${}^{NaB}\Delta E = 0$. The other electrochemical cell arrangement of high importance is the one where the compositions of each compartment approach the pure elements (i.e. $Y_{Na^+}^{anode}, Y_{Na^-}^{anode} \rightarrow 1$ and $Y_{Na^+}^{cathode}, Y_{Na^-}^{cathode} \rightarrow 0$) and it is herein defined that ${}^{NaB}\Delta E \rightarrow {}^{NaB}\Delta E^\circ \rightarrow -ZTC^\circ$. Electrochemical cells where the forward and reverse of the same amphoteric half-reaction occurs in its compartments are concentration cells that implicate mixing processes. As it will be shown later, however, the same is true for the hydrolysis reactions.

In what follows isothermal, isobaric, equivalent, elemental, ternary composition triangles and analogous higher order composition domains are constructed out of common-ion sub-binary composition

lines, non-common-ion elemental binary composition lines, quasi-common-ion sub-binary composition lines (2.2.5), and mixtures thereof.

2.2 Isothermal, isobaric, equivalent, elemental, ternary composition triangles

Five types of isothermal, isobaric, elemental, equivalent ternary composition triangles are shown in Fig. 6; they include: (A) composition triangles not having an obvious compound on any of its three elemental binary composition lines or within its ternary region; (B) composition triangles that have an obvious compound on one of its three elemental binary composition lines but none within its ternary regions; (C) composition triangles having an obvious compound on two of its three elemental binary composition lines but none within its ternary regions; (D) composition triangles having obvious compounds on all three of its elemental binary composition lines but none within its ternary regions; and (E) systems having one obvious compound on one of its elemental binary composition lines and one within its ternary region. For the processes given in the previous section to be graphically expressed under this electrochemical reaction formalism, later, the Na-B-H-O composition tetrahedron, which itself can be divided into five sub-quaternary composition figures that are defined by a maximum of two of the possible four amphoteric half-reactions, will be constructed from two type-C, one type-D, and one type-E composition triangles

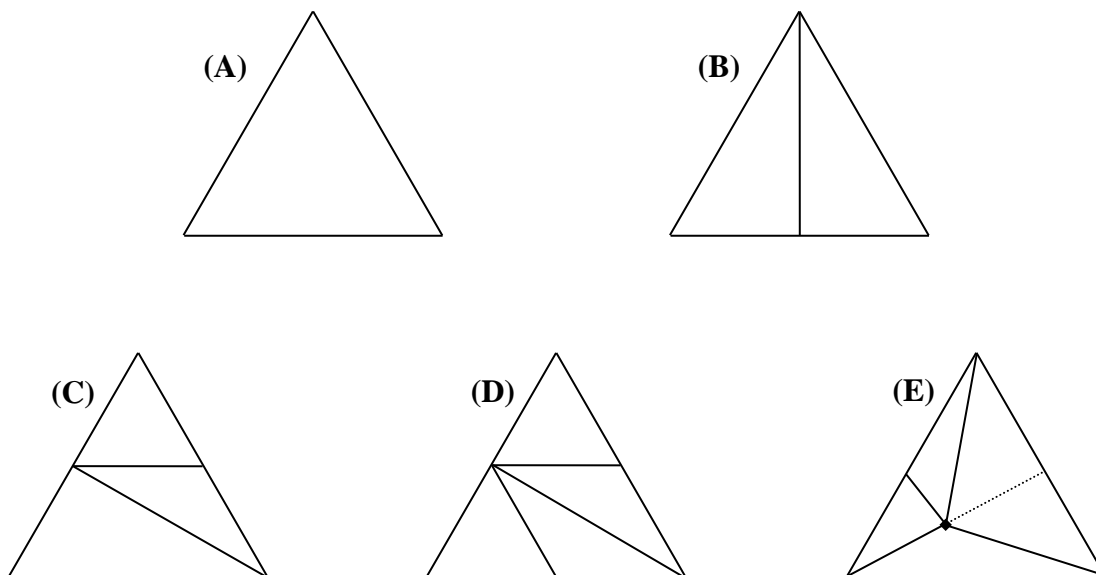


Fig. 6 Five types of isothermal, isobaric, equivalent, elemental, ternary composition triangles

2.2.1 Type-A, isothermal, isobaric, equivalent, elemental, ternary composition triangles

At elevated temperatures (>900 K) and standard pressure, all of the Na-B-H system's elemental binary composition lines may be regarded as non-common-ion (2.1). Although ternary mixtures are comprised of six ions (B^{3+} , B^{3-} , Na^+ , Na^- , H^+ , and H^-), the conditions: $Y_{B^{3+}} = Y_{B^{3-}}$, $Y_{Na^+} = Y_{Na^-}$, $Y_{H^+} = Y_{H^-}$, $Y_{H^+} + Y_{B^{3+}} + Y_{Na^+} = 1$, and $Y_{H^-} + Y_{B^{3-}} + Y_{Na^-} = 1$ makes it so that composition is defined when two different elements have one of their EEIFs specified so that composition may be plotted on a Gibbs (equilateral) composition triangle using any one of the eight EEIF coordinate permutations

$$\left(Y_{Na^+}, Y_{H^+}, Y_{B^{3+}} \right), \quad \left(Y_{Na^-}, Y_{H^+}, Y_{B^{3+}} \right), \quad \left(Y_{Na^+}, Y_{H^-}, Y_{B^{3+}} \right), \quad \left(Y_{Na^-}, Y_{H^-}, Y_{B^{3+}} \right), \quad \left(Y_{Na^+}, Y_{H^-}, Y_{B^{3-}} \right), \\ \left(Y_{Na^-}, Y_{H^-}, Y_{B^{3-}} \right), \left(Y_{Na^+}, Y_{H^+}, Y_{B^{3-}} \right), \text{ or } \left(Y_{Na^+}, Y_{H^+}, Y_{B^{3-}} \right).$$

From the assumption that obvious compounds are nonexistent within the overall composition triangle, as was the case for Na-B system, if a galvanic cell is constructed with an inert solid ion electrolyte having pure conductance for only one of the six ions, the processes at each electrode are the forward (reduction) and reverse (oxidation) of the amphoteric half-reaction that implicates that ion.

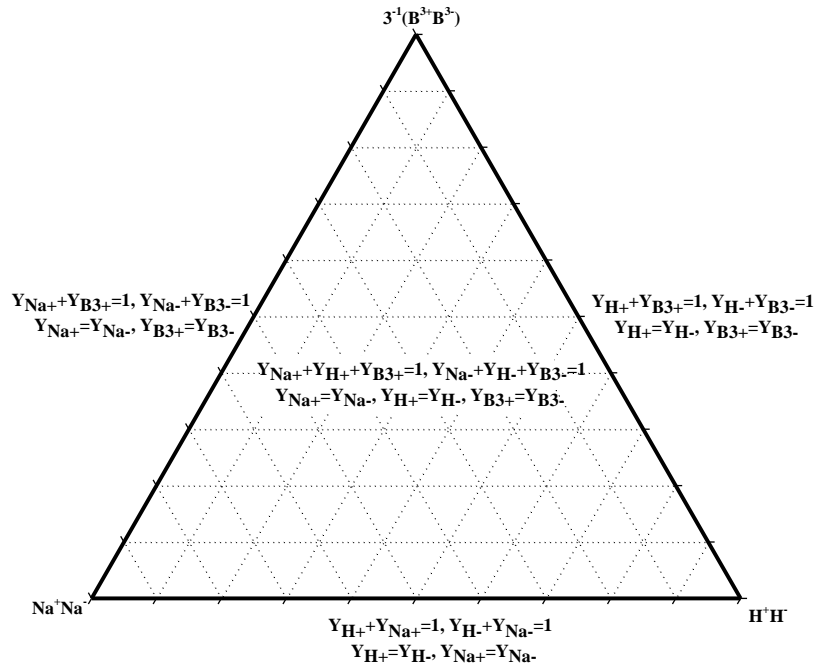


Fig. 7 Type A, isothermal, isobaric, equivalent, elemental, ternary composition triangle for Na-B-H system at temperatures greater than 873 °K and at or below ambient pressure.

So long as the temperature is above and the pressure is below the levels required for $NaBH_4$'s and NaH 's decomposition, any point within the ternary composition triangle may be viewed as one of the possible compositions of one of a perfect electrochemical cell's independent compartments. Because no obvious compounds exist, as given in (Eq. 37), the MNE takes a similar form to the one given for the elemental binary composition line for which no obvious compound form (Eq. 36). That is, in all cases the ratio of the chosen amphoteric element's EEIFs is, again, equal to unity, and the choice of which amphoteric element's EEIFs are to be used in the MNE is determined by the choice/availability of the solid ion electrolyte.

$$NaBH \Delta E = -ZT \left(\ln \left(\frac{Y_{Na^+}^{1/2}}{Y_{Na^-}^{1/2}} \right)^{B^{3+}, H^+, Na^+ / Na^-, H^-, B^{3-}} + \ln \left(\frac{Y_{Na^-}^{1/2}}{Y_{Na^+}^{1/2}} \right)^{B^{3+}, H^+, Na^+ / Na^-, H^-, B^{3-}} + C \right) \quad (37)$$

2.2.2 Type-B, isothermal, isobaric, equivalent, elemental, ternary composition triangles

At ambient pressure and temperatures ≥ 700 °K, elemental mixtures of lithium, boron, and hydrogen may be graphically represented by a type-B, isothermal, isobaric, equivalent, elemental, ternary

composition triangle (Fig. 8). LiH is the only obvious compound; so, like the H-O composition line (Fig. 5), the Li-H composition line is divided at its midpoint into two common-ion, sub-binary composition lines. The B-H and B-Li elemental binaries are non-common-ion analogues of the Na-B composition line (Fig. 6). Both of the sub-ternary composition triangles (I and II) are herein defined as isothermal, isobaric, five-ion, equivalent, elemental, sub-ternary composition triangles. Along with (Eq. 18), all sub-ternary mixtures are beholden to the condition: $Y_{B^{3+}} = Y_{B^{3-}}$. Furthermore, because of the relation: $Y_{Li^+} = Y_{H^-}$, the B-LiH composition line bears likeness to elemental, non-common-ion binary composition lines. Li-B-LiH ($B^{3+}, Li^+/Li^-, B^{3-}, H^-$; I) mixtures are defined by seven EEIF pair permutations (i.e. $(Y_{B^{3+}}, Y_{Li^-})$, $(Y_{B^{3+}}, Y_{H^-})$, (Y_{Li^+}, Y_{Li^-}) , (Y_{Li^+}, Y_{H^-}) , $(Y_{Li^-}, Y_{B^{3-}})$, (Y_{Li^-}, Y_{H^-}) , and $(Y_{B^{3-}}, Y_{H^-})$) that may be plotted in a Gibbs (equilateral) triangle using either $(Y_{B^{3+}}, Y_{Li^-}, Y_{H^-})$ or $(Y_{B^{3+}}, Y_{Li^-}, Y_{H^-})$ EEIF coordinates. Analogous permutations for B-H₂-LiH ($Li^+, B^{3+}, H^+/H^-, B^{3-}$; II) sub-ternary mixtures are easily deduced.

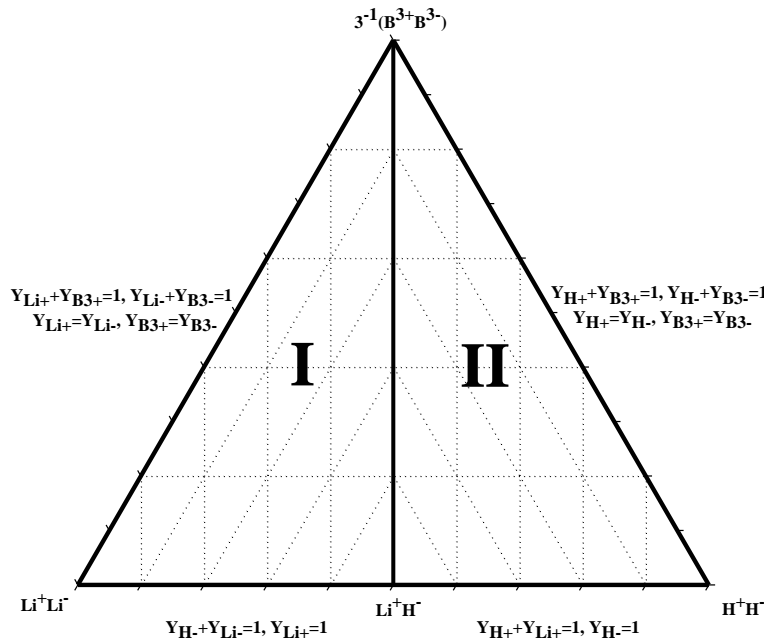


Fig. 8 Type-B, isothermal, isobaric, equivalent, elemental, ternary composition triangle represented by the Li-B-H system at elevated temperatures (e.g. >700 °K) and ambient pressure

With regards to perfect galvanic cells, if the anode (I) and cathode (II) compartments are electrically connected by a solid lithium cation electrolyte, then, due to ionic current flow and simultaneous electro-oxidation of Li^- to Li^+ in (I) and electro-reduction of H^+ to H^- in (II), LiH will accumulate in (II). For, if the anode (I) and cathode (II) compartments are in electrical contact via a solid hydrogen anion electrolyte (SHAE) [48], then the passage of ionic current will lead to the formation of LiH in (I). In other words, the solid ion electrolyte must be purely conductive to either Li^+ or H^- (i.e. the ternary mixture's obvious compound's ionic constituents), and the direction of the amphoteric half-reactions at their respective electrodes will be the same regardless of which solid ion electrolyte is chosen (see Table 2). It is shown in the MNE (Eq. 38) that, due to the aforementioned constraints, either sub-ternary system's composition may be defined by the ratio of its corresponding amphoteric element's EEIFs. Given that the temperature and pressure are both specified, the potential difference measured between the two compartments ($^{I-II} \Delta E$) is a function of the standard potential difference of LiH formation ($^{LiH} \Delta E^\circ$) which is measured as $Y_{Li^+}, Y_{Li^-} \rightarrow 1$ in (I) and $Y_{H^+}, Y_{H^-} \rightarrow 1$ in (II).

$$I/II \Delta E = {}^{LiH} \Delta E^\circ - ZT \left(\ln \left(\frac{Y_{Li^+}^{1/2}}{Y_{Li^-}^{1/2}} \right)^{B^{3+}, Li^+ / Li^-, B^{3-}, H^-} + \ln \left(\frac{Y_{H^-}^{1/2}}{Y_{H^+}^{1/2}} \right)^{B^{3+}, Li^+, H^+ / H^-, B^{3-}} + C \right) \quad (38)$$

In regards to perfect galvanic cells, if both the anolyte and catholyte compositions are comprised of mixtures belonging to sub-ternary system II, then a solid ion electrolyte with a transport number of unity for either one of the ions belonging to H₂—the system's amphoteric element—would be required, and the forward and reverse of H₂'s amphoteric half-reaction (Eq. 22) would occur at both electrodes. The direction of the internal flow of ionic current will be the same regardless of which solid ion electrolyte is used, but the type of solid ion electrolyte will determine which compartment is anodic and which compartment is cathodic. For example, if compartment (a) contained more H₂ than compartment (b) and a SHCE were employed, then compartment (a) would be anodic as H⁻ would be electro-oxidized to H⁺, compartment (b) would be cathodic as H⁺ would be electro-reduced to H⁻, and the internal ionic current (H⁺) would flow from (a) to (b). Alternatively, if, once again, compartment (a) contained more H₂ than compartment (b) and a SHAE were employed, then compartment (a) would be cathodic as H⁺ would be electro-reduced to H⁻, and compartment (b) would be anodic as H⁻ would be electro-oxidized to H⁺, and the internal ionic current (H⁻) would again flow from (a) to (b). The same reasoning could be applied to sub-ternary system I. However, due to lithium's low electron-affinity it does not seem plausible that a solid lithium anion electrolyte will ever be realized.

For electrochemical mixing studies, taking sub-ternary composition triangle II for example, with the exception of the number of so-considered ions, the MNE may be presented in the form given by (Eq. 39). It differs from (Eq. 36) and (Eq. 37) because the ratio of the amphoteric element's EEIFs is only unity along the H₂-B composition line; hence, when the anode and cathode compartments' compositions lie within the sub-ternary region, the logarithmic terms carrying the ratios of the amphoteric element's EEIFs are not equal to zero.

$$II/II \Delta E = -ZT \left(\ln \left(\frac{Y_{H^+}^{1/2}}{Y_{H^-}^{1/2}} \right)^{B^{3+}, Li^+, H^+ / H^-, B^{3-}} + \ln \left(\frac{Y_{H^-}^{1/2}}{Y_{H^+}^{1/2}} \right)^{B^{3+}, Li^+, H^+ / H^-, B^{3-}} + C \right) \quad (39)$$

2.2.3 Type-C, isothermal, isobaric, equivalent, elemental, ternary composition triangles

Over a wide range of temperature and pressure, the graphical representation of Na-B-O mixtures composition can be accomplished via a type-C isothermal, isobaric, equivalent, elemental, ternary composition triangle (Fig. 9). Roman numerals denote the three principal sub-ternary composition triangles. The Na-B system was previously discussed (2.1). Like the H-O elemental binary system, both the Na-O and B-O systems contain two common-ion sub-binary composition lines. (Na⁺/Na⁻, O²⁻ and Na⁺, O²⁺/O²⁻, and B³⁺/B³⁻, O²⁻ and B³⁺, O²⁺/O²⁻, respectively.) Due to space constraints, the Na₂O-B₂O₃ sub-binary composition line's *less obvious compounds* are not shown.

I (Na₂O-B₂O₃-O₂) is comprised of three cations (B³⁺, Na⁺, O²⁺) and one anion (O²⁻) and is herein defined as an isothermal, isobaric, equivalent, elemental, additive, sub-ternary composition triangle; its perimeter is comprised of three common-ion, sub-binary composition lines where Y_{O²⁻} = 1 and its ternary region is defined by Y_{O²⁻} = 1 and Y_{O²⁺} + Y_{Na⁺} + Y_{B³⁺} = 1. Hence, the composition is defined by two cationic EEIFs, and a Gibbs composition triangle having ternary coordinates (Y_{O²⁺}, Y_{Na⁺}, Y_{B³⁺}) unambiguously specifies composition. The half-reaction given by (Eq. 24) is sufficient for the description of the possible electrochemical processes occurring within the composition domain. But because Y_{O²⁻} = 1

, when writing the MNE, the ratio of the amphoteric element's EEIF (i.e. $Y_{O^{2+}}/Y_{O^{2-}}$) does not specify the system's composition; rather, an additional cationic EEIF must also be specified.

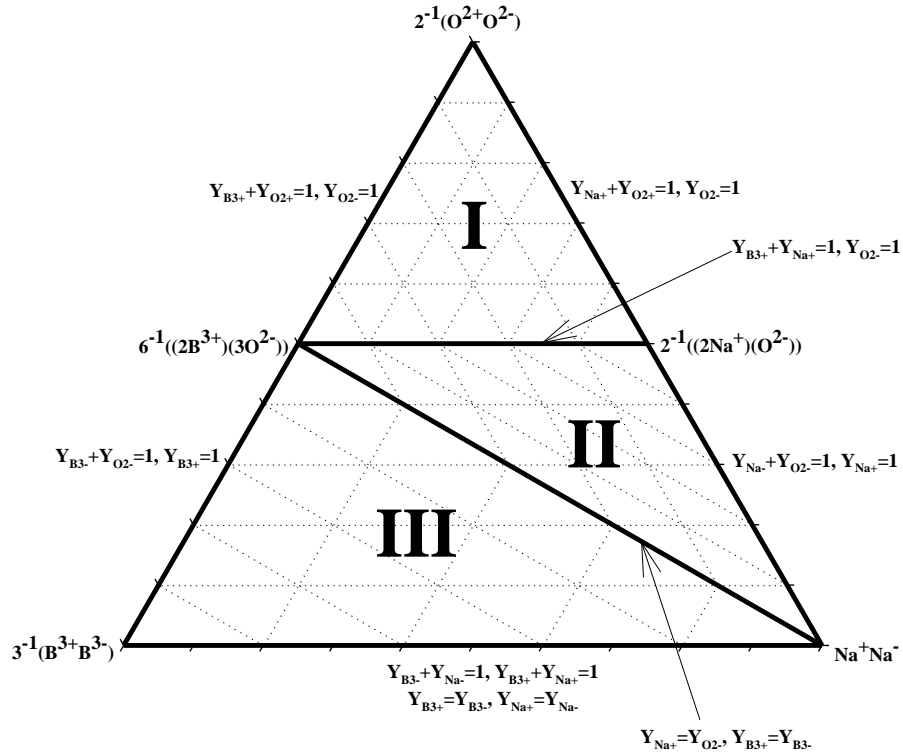
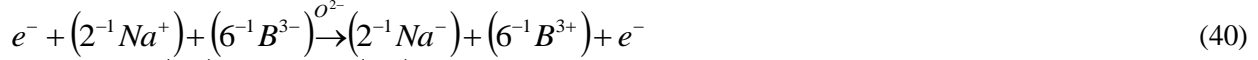


Fig. 9 Type C, isothermal, isobaric, equivalent, elemental ternary composition triangle for the Na-B-O system

II (Na-Na₂O-B₂O₃) is defined as an isothermal, isobaric, equivalent, elemental, reciprocal ternary composition half-square; its two-cation, two-anion mixtures ($B^{3+}, Na^+/Na^-, O^{2-}$) are bound by the conditions: $Y_{Na^+} + Y_{B^{3+}} = 1$, $Y_{O^{2-}} + Y_{Na^-} = 1$, and the inequality: $Y_{Na^-} \leq Y_{Na^+}$; its perimeter is constructed from two common-ion ($Na^+, B^{3+}/O^{2-}$ and $Na^+/Na^-, O^{2-}$) and one non-common-ion ($B^{3+}, Na^+/Na^-, O^{2-}$) binary composition lines. By specifying one cationic and one anionic EEIF, the system's composition is arbitrarily but uniquely defined and can be graphically represented with Cartesian co-ordinates (i.e. (Y_{Na^+}, Y_{Na^-}) , $(Y_{Na^+}, Y_{O^{2-}})$, $(Y_{B^{3+}}, Y_{Na^-})$, or $(Y_{B^{3+}}, Y_{O^{2-}})$). The amphoteric half-reaction given by (Eq. 33) generally expressed the electrochemical processes for which these sub-ternary mixtures are capable of.

III (Na-B-B₂O₃) is another example of an isothermal, isobaric, five-ion, equivalent, elemental, sub-ternary composition triangle (2.2.2); its three-anion, two-cation mixtures ($Na^+, B^{3+}/B^{3-}, Na^-, O^{2-}$) have for relationships $Y_{B^{3+}} + Y_{Na^+} = 1$, $Y_{B^{3-}} + Y_{Na^-} + Y_{O^{2-}} = 1$, and $Y_{Na^+} = Y_{Na^-}$. The plotting of composition is facilitated by a Gibbs (equilateral) composition triangle using either $(Y_{Na^+}, Y_{B^{3-}}, Y_{O^{2-}})$ or $(Y_{Na^-}, Y_{B^{3-}}, Y_{O^{2-}})$ EEIF coordinates. If a galvanic cell of the kind under consideration (2.1) has its electrochemical potential measured with respect to either of the two other principal equivalent composition triangles (i.e. I or II), the forward or reverse of the amphoteric half-reaction given by (Eq. 33) generally describes the electrochemical process.

Equivalent processes such as the one causing the triangulation of the Na-Na₂O-B₂O₃-B composition square are defined as reciprocal-formation processes; they are expressions of the logical summation of two amphoteric half-reactions where a *supporting ion* cancels itself in the equivalent chemical reaction. Evidently, the oxidation states of the elements in the obvious product and reactant compounds must be known. In the present case, sodium and boron evidently have positive character in their respective metal oxide compounds; hence, O²⁻ is the supporting ion in the overall process. Then, from the logical summation of (Eq. 32) and (Eq. 33) we obtain (Eq. 40), and consequently $\Delta G^{\circ eq}$ (Eq. 41), where again $\Delta G^{\circ eq}$ is the free energy for the reaction on a one Coulomb basis that can be calculated from the concerned independent variable components' absolute free energies at a specific temperature and a specific pressure.

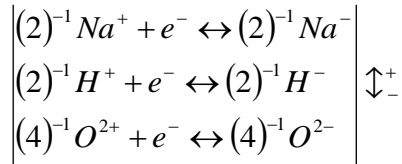


If a perfect electrochemical cell were conceivable, as the so-considered ionic mixtures of the anode (III) and the cathode (II) compartments approach that of pure boron (i.e. $Y_{B^{3-}}, Y_{B^{3+}} \rightarrow 1$) and Na₂O (i.e. $Y_{Na^{+}} \rightarrow 1, Y_{O^{2-}} \rightarrow 1$), respectively, $^{III/II} \Delta E \rightarrow -ZT \Delta G^{\circ eq}$.

$$(\phi^{Cu} - \phi^{Cu'}) = ^{III/II} \Delta E = -ZT \left(\ln \left(\frac{Y_{Na^{-}}^{1/2}}{Y_{Na^{+}}^{1/2}} \right)^{II} + \ln \left(\frac{Y_{B^{3+}}^{1/6}}{Y_{B^{3-}}^{1/6}} \right)^{III} + C \right)$$

2.2.4 Type D, isothermal, isobaric, equivalent, elemental, ternary composition triangles

Type-D, isothermal, isobaric, equivalent, elemental, ternary composition triangles facilitate the description of the automotive fuel-cycles discussed in (1.1). The Na-O-H system constitutes itself as a type-D system at temperatures less and pressures greater than what is required for NaH's decomposition. The electro-negativity series for this set of elements is unarguably Na<H<O thus its electrochemical series may be expressed by the three amphoteric half-reactions:



For the electrochemical compound formation reactions pertaining to Na-O (Na₂O) and Na-H (NaH) elemental binary composition lines, the same procedure as the one used in (2.1) results in analogous MNEs (Eq. 31). Sketches of their perfect electrochemical cells constructed with their respective inert solid ion electrolytes are shown in Table 2 using both conventional and amphoteric notations. The standard binary compound formation potentials are noted by $^{ONa} \Delta E^{\circ}$ and $^{NaH} \Delta E^{\circ}$ which can be determined from the independently variable components' absolute free energy data.

$$\begin{aligned}
{}^{ONa}\Delta E^\circ(T) &= F^{-1}\left((4)^{-1}\mu_{O_2}^\circ + (2)^{-1}\mu_{Na^+}^\circ - (4)^{-1}\mu_{O_2}^\circ - (2)^{-1}\mu_{Na^+}^\circ\right) \\
&= F^{-1}\left((2)^{-1}\mu_{Na_2}^\circ + (4)^{-1}\mu_{O_2}^\circ - (2)^{-1}\mu_{Na_2O}^\circ\right) = F^{-1}\left(-{}^{ONa}\Delta G^{\circ eq}(T)\right) \\
{}^{NaH}\Delta E^\circ(T) &= F^{-1}\left((2)^{-1}\mu_{Na^+}^\circ + (2)^{-1}\mu_{H^-}^\circ - (2)^{-1}\mu_{Na^+}^\circ - (2)^{-1}\mu_{H^+}^\circ\right) \\
&= F^{-1}\left((2)^{-1}\mu_{H_2}^\circ + (2)^{-1}\mu_{Na_2}^\circ - \mu_{NaH}^\circ\right) = F^{-1}\left(-{}^{NaH}\Delta G^{\circ eq}(T)\right)
\end{aligned}$$

For the sake of comparison, the isothermal, isobaric Na-H-O elemental ternary composition triangle is shown on the basis of atomic percentage (Fig. 10(a)) and EEIFs (Fig. 10(b)). The composition domain is divided into three sub-ternary composition figures (Roman numerals) that may be regarded as regions of ionic stability where only one of the three amphoteric half-reactions is possible. These include two elemental, equivalent additive, Gibbs (equilateral) sub-ternary composition triangles: I ($O^{2-}, H^+, Na^+/Na^+$) and III ($Na^+, H^+, O^{2+}/O^{2-}$), and a herein defined elemental, equivalent, reciprocal ternary composition square: II ($Na^+, H^+/H^-, O^{2-}$; also shown in Fig. 10(c)). Again, the number of electrochemical half-reactions in each region is reduced to one and are given by (Eq. 33), (Eq. 23), and (Eq. 22), respectively.

Table 2 Sketches of perfect galvanic cells for the Na-H-O system's obvious compounds formations given in conventional and amphoteric (bottom panels) notation.

| $Na + (4)^{-1}O_2 = (2)^{-1}Na_2O$ <small>$NaO \Delta E^\circ$</small> | $Na + (2)^{-1}H_2 = NaH$ <small>$NaH \Delta E^\circ$</small> | $(4)^{-1}O_2 + (2)^{-1}H_2 = (2)^{-1}H_2O$ <small>$OH \Delta E^\circ$</small> |
|--|--|---|
| <div style="display: flex; justify-content: space-around; align-items: center;"> <div style="text-align: center;"> $Na = Na^+ + e^-$ $e^- + (4)^{-1}O_2 + Na^+ = (2)^{-1}Na_2O$ </div> <div style="text-align: center;"> $(2)^{-1}H^+ + Na = NaH + e^-$ $e^- + (2)^{-1}H_2 = H^+$ </div> <div style="text-align: center;"> $(2)^{-1}H_2 = (2)^{-1}H^+ + e^-$ $(2)^{-1}H^+ + (4)^{-1}O_2 + e^- = (2)^{-1}H_2O$ </div> </div> | <div style="display: flex; justify-content: space-around; align-items: center;"> <div style="text-align: center;"> $(2)^{-1}O^{2-} + Na = (2)^{-1}Na_2O + e^-$ $e^- + (4)^{-1}O_2 = (2)^{-1}O^{2-}$ </div> <div style="text-align: center;"> $Na = Na^+ + e^-$ $e^- + Na^+ + (2)^{-1}H_2 = NaH$ </div> <div style="text-align: center;"> $(2)^{-1}H_2 + (2)^{-1}O^{2-} = (2)^{-1}H_2O + e^-$ $(4)^{-1}O_2 + e^- = (2)^{-1}O^{2-}$ </div> </div> | <div style="display: flex; justify-content: space-around; align-items: center;"> <div style="text-align: center;"> $(2)^{-1}Na^+ = (2)^{-1}Na^+ + e^-$ $(4)^{-1}O^{2+} + e^- = (4)^{-1}O^{2-}$ </div> <div style="text-align: center;"> $(2)^{-1}Na^+ = (2)^{-1}Na^+ + e^-$ $(2)^{-1}H^+ + e^- = (2)^{-1}H^-$ </div> <div style="text-align: center;"> $(2)^{-1}H^- = (2)^{-1}H^+ + e^-$ $(4)^{-1}O^{2+} + e^- = (4)^{-1}O^{2-}$ </div> </div> |

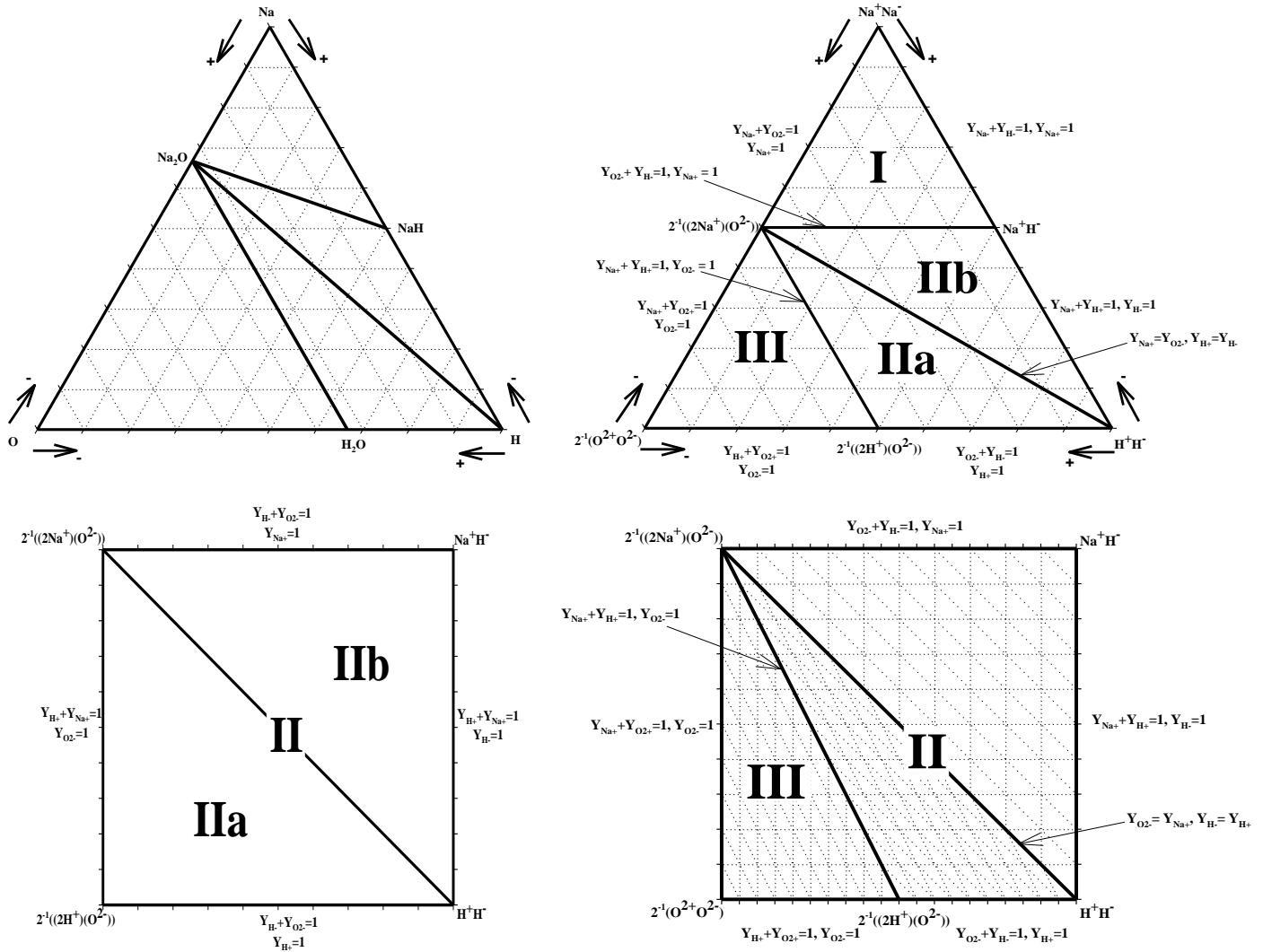
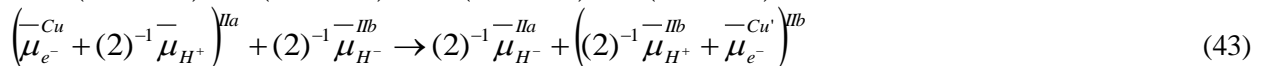
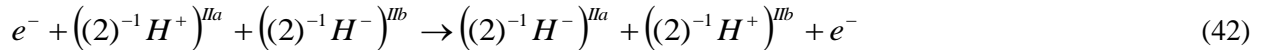


Fig. 10 Type-D, isothermal, isobaric, elemental, ternary composition triangle for the Na-O-H system for pressures and temperatures above and below NaH's decomposition shown on the basis of (a) atomic mole percentages and (b) EEIFs; (c) Na₂O-NaH-H₂O-H₂ (Na⁺, H⁺/H⁻, O²⁻) equivalent, elemental, reciprocal, sub-ternary composition square (d) combined with the O₂-Na₂O-H₂O (Na⁺, H⁺, O²⁻/O²⁻) equivalent, elemental, additive sub-ternary composition triangle shown on the basis of EEIFs.

Assuming that a perfect electrochemical cell's compartments are separated from each other by an appropriate solid ion electrolyte that allows for the passage of only one ion, if a potential difference is measured between two electrode compartments that both contain mixtures from the same additive sub-ternary system (i.e. I or III), its magnitude is related to the Gibbs energy of mixing. This is also the case if both of the two compartments contain mixtures in IIa or IIb. However, if one compartment contains a mixture from IIa and the other a mixture from IIb, the measured potential difference will be proportional to the hydrolysis reaction (Eq. 6).



*Corresponding author Tel.: +1 819 821 8000ext63238; fax: +1 819 821 7095
E-mail: danielcalabretta@gmail.com

$$(\phi^{Cu} - \phi^{Cu'})_{=Na^+, H^+ / H^-, O^{2-}} \Delta E = {}^{IIa} / {}^{IIb} \Delta E = -ZT \left(\ln \left(\frac{Y_{H^-}^{1/2}}{Y_{H^+}^{1/2}} \right)^{IIa} + \ln \left(\frac{Y_{H^+}^{1/2}}{Y_{H^-}^{1/2}} \right)^{IIb} + C \right) \quad (44)$$

As shown in Fig. 11 if the hydrolysis of NaH (Eq. 6) via a perfect galvanic cell is considered, it is found that molecular H₂ will be produced at both electrodes as H⁺ from H₂O and H from NaH will simultaneously be electro-reduced and electro-oxidized at the cathode and anode, respectively. Evidently, either Na⁺ or O²⁻ could carry the internal current. From (Eq. 42) and (Eq. 43), the MNE for this process is given by (Eq. 44).

If $(Y_{H^+})^{IIa}, (Y_{H^-})^{IIb} \rightarrow 1$ and $(Y_{H^-})^{IIa}, (Y_{H^+})^{IIb} \rightarrow 0$, the compositions of compartments IIa (H₂-H₂O-Na₂O) and IIb (H₂-NaH-Na₂O) approach that of pure H₂O and NaH, respectively, and the potential difference $(\Delta E)_{=Na^+, H^+ / H^-, O^{2-}} \xrightarrow{Hydrolysis} \Delta E^\circ$ would approach that of the standard hydrolysis reaction (absolute free energies).

$$\begin{aligned} & {}_{Na^+, H^+ / H^-, O^{2-}} \Delta E \xrightarrow{Hydrolysis} \Delta E^\circ = {}^{ONa} \Delta E^\circ + {}^H E^\circ - {}^{OH} \Delta E^\circ - {}^{NaH} \Delta E^\circ = {}^{ONa} \Delta E^\circ - {}^{OH} \Delta E^\circ - {}^{NaH} \Delta E^\circ \\ & = F^{-1} \left((2)^{-1} \mu_{Na_2}^\circ + (4)^{-1} \mu_{O_2}^\circ - (2)^{-1} \mu_{Na_2O}^\circ - (2)^{-1} \mu_{H_2}^\circ - (4)^{-1} \mu_{O_2}^\circ + (2)^{-1} \mu_{H_2O}^\circ - (2)^{-1} \mu_{H_2}^\circ - (2)^{-1} \mu_{Na_2}^\circ + \mu_{NaH}^\circ \right) \\ & = F^{-1} \left((2)^{-1} \mu_{H_2O}^\circ + \mu_{NaH}^\circ - (2)^{-1} \mu_{Na_2O}^\circ - \mu_{H_2}^\circ \right) = F^{-1} \left(-{}^{Hydrolysis} \Delta G^{oeq} \right) \end{aligned}$$

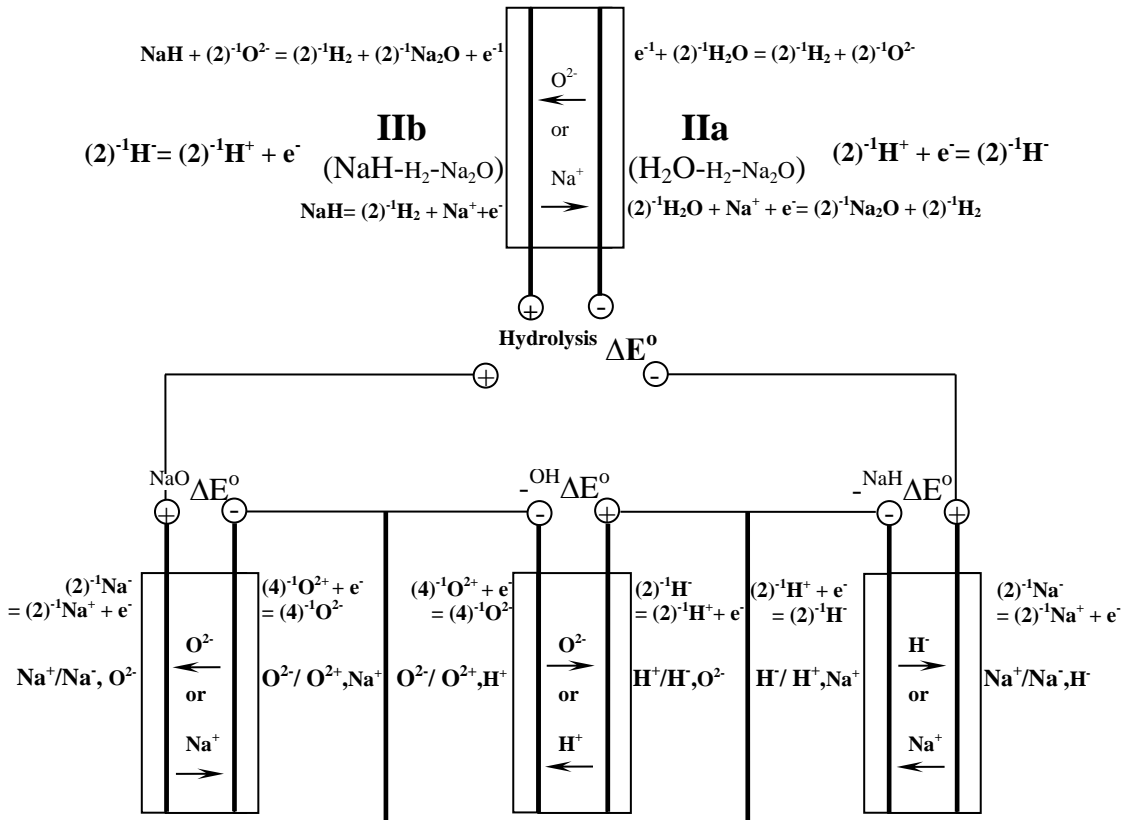
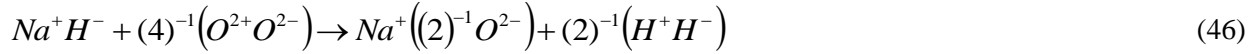


Fig. 11 Sketch showing the equivalence between perfect galvanic cells including hydrolysis (top) and obvious compound formation (bottom; Table 2)

Sub-ternary composition triangles II and III are combined in Fig. 10(d) in order to illustrate the overall composition domain (Na⁺-O-H) that is required for perfect galvanic combustion cells. An analogous composition square could be given if sub-ternary systems I and II were combined (O²⁻-Na-H). In the former case, assuming that the two compartments are completely isolated from each another by a SOAE or SSCE, and that each electrode is in contact with mixtures of different stability region, two different amphoteric half-reactions will occur (i.e. (Eq. 22) and (Eq. 23)).

The combustion of NaH is given in conventional notation (Eq. 45) and amphoteric notation (Eq. 46). Upon cancellation of the redundant species (Eq. 47), we find that the process resembles that of water formation (Eq. 21). However, in this case, Na⁺ acts as a cationic support for both H⁻ and O²⁻ anions, and the effect of its presence on the system is explicitly accounted for by expressing the composition of each the perfect galvanic cell's compartments as the ratio of the two EEIFs of the ionic stability zone's electro-active species in the MNE (Eq. 48), which closely resembles (Eq. 30). Obviously, $(Y_{H^+})^{III}$ may not be equal to unity and in order to assign the catholyte's composition either Y_{Na^+} or Y_{H^+} must be specified.



$${}^{II/III} \Delta E = {}^{OH} \Delta E^\circ - ZT \left(\ln \left(\frac{Y_{H^+}^{1/2}}{Y_{H^-}^{1/2}} \right)^{II} + \ln \left(\frac{Y_{O^{2-}}^{1/4}}{Y_{O^{2+}}^{1/4}} \right)_{Y_{Na^+} \text{ or } Y_{H^+}}^{III} + C \right) \quad (48)$$

If NaH is absent in the anode compartment, then only water formation can occur, and as $(Y_{O^{2-}}, Y_{O^{2+}} \rightarrow 1)^{III}$ and $(Y_{H^+}, Y_{H^-} \rightarrow 1)^{II}$, then ${}^{II/III} \Delta E \rightarrow {}^{OH} \Delta E^\circ$. The measured potential difference will approach that of the standard potential of combustion (${}^{Combustion} \Delta E^\circ$) as $(Y_{H^+} \rightarrow 0, Y_{H^-} \rightarrow 1)^{II}$ and $(Y_{O^{2-}}, Y_{O^{2+}})^{III} \rightarrow 1$, as the so-considered ionic mixtures representing the catholyte and anolyte compartments approach that of pure NaH (II) and O₂ (III), respectively.

$$\begin{aligned} {}^{II/III} \Delta E &\rightarrow {}^{Combustion} \Delta E^\circ = {}^{ONa} \Delta E^\circ + {}^H E^\circ - {}^{NaH} \Delta E^\circ - {}^O E^\circ = {}^{ONa} \Delta E^\circ - {}^{NaH} \Delta E^\circ \\ &= F^{-1} \left((2)^{-1} \mu_{Na_2}^\circ + (4)^{-1} \mu_{O_2}^\circ - (2)^{-1} \mu_{Na_2O}^\circ - (2)^{-1} \mu_{H_2}^\circ - (2)^{-1} \mu_{Na_2}^\circ + \mu_{NaH}^\circ \right) \\ &= F^{-1} \left((4)^{-1} \mu_{O_2}^\circ + \mu_{NaH}^\circ - (2)^{-1} \mu_{Na_2O}^\circ - (2)^{-1} \mu_{H_2}^\circ \right) = F^{-1} \left(-{}^{Combustion} \Delta G^{eq} \right) \end{aligned}$$

Fig. 12 illustrates the equivalence between ${}^{Combustion} \Delta E^\circ$ and the formation type galvanic cells (Table 2) in series with the individual cell polarities arranged so that their signs correspond to ${}^{Combustion} \Delta E^\circ = {}^{ONa} \Delta E^\circ - {}^{NaH} \Delta E^\circ$. By substitution it is found that ${}^{Combustion} \Delta E^\circ = {}^{Hydrolysis} \Delta E^\circ + {}^{OH} \Delta E^\circ$ and that electrochemical complete oxidation of metal hydrides, including the carbon hydrides, may be achieved by constructing the corresponding galvanic cells in series. Moreover, for complete oxidation, we find that ${}^{CO} \Delta E^\circ = {}^{Combustion} \Delta E^\circ + {}^{OH} \Delta E^\circ = {}^{Hydrolysis} \Delta E^\circ + 2 {}^{OH} \Delta E^\circ$.

Many groups have attempted to do ERCO in aqueous solutions without success. The reasons for this, although not clearly stated in the open literature, are obvious from classical thermodynamic considerations. As the potential for water electrolysis (${}^{WE} \Delta E^\circ = -1.23$ V at STP) has an absolute value

that is clearly less than that of ERC ($^{ERC} \Delta E^\circ = ^{WE} \Delta E^\circ + ^{ERH} \Delta E^\circ$), attempts to perform ERC in aqueous solutions saturated with metal oxides/hydroxides will result in water electrolysis until solids form such that there can be no appreciable mass transfer of metal oxides/hydroxides to the catholyte-cathode interface. And even if there were, any formation of metal hydrides in the catholyte would, with time, subsequently hydrolyze if water or hydroxides are present. Although $^{ERH} \Delta E^\circ \approx -0.3$ V (for the Na-H-O system at STP) has an absolute value that is considerably less than that of $^{WE} \Delta E^\circ$, its execution is impossible in aqueous solution, since, again, the metal hydride would tend to hydrolyze. Moreover, due to mass transfer considerations, simple ERCO processes could only be practically realized if one of the two necessary electrolytic processes (i.e. ERH or ERC) has in its cathode compartment a liquid, anhydrous mixtures akin to those found in the elemental ternary reciprocal composition square IIb (Fig. 10(c)). At the time of this writing, no reports on attempts to test these types of electrolytic cells exist.

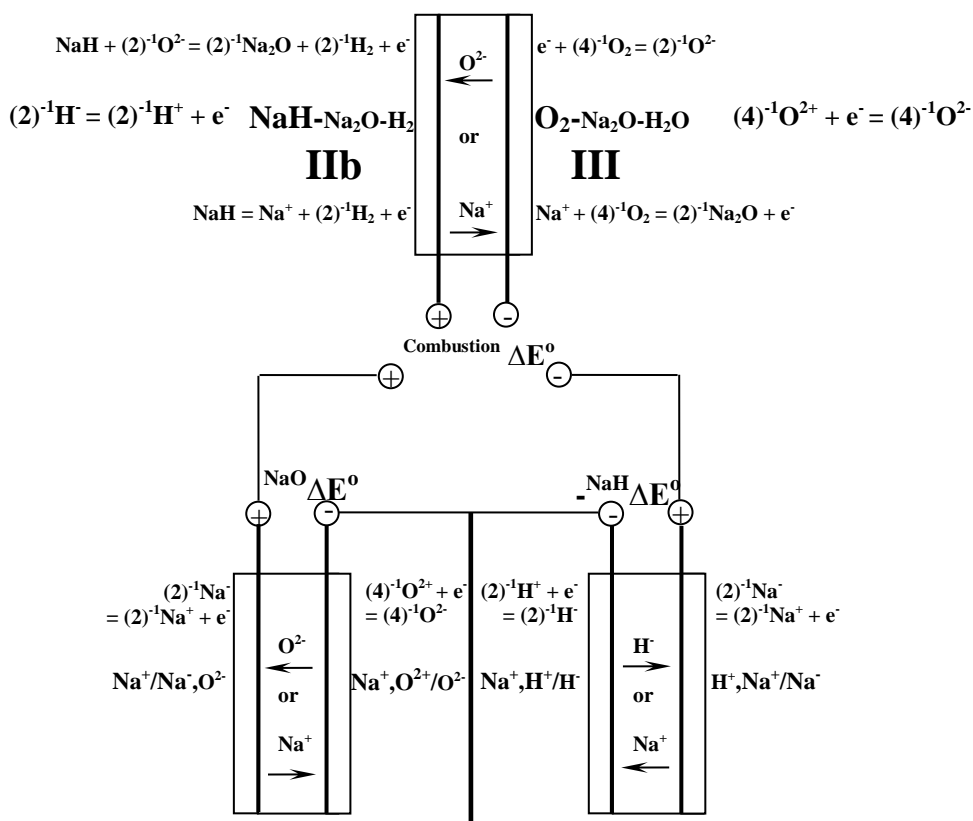


Fig. 12 Sketch showing the equivalence between perfect combustion (top) and obvious compound formation (bottom; Table 2) galvanic cells

2.2.5 Type-E, isothermal, isobaric, equivalent, elemental, ternary composition triangles

At temperatures and pressures where NaBH_4 and NaH are stable, and B_2H_6 is unstable (from decomposition), elemental mixtures of Na, B, and H may be represented by the ternary composition (equilateral) triangle shown in Fig. 13 (i.e. a type-E elemental, equivalent, ternary composition triangle). NaBH_4 , the stable ternary compound, is positioned at the midpoint of the line that extends from pure H_2 and the Na-B elemental binary composition line where $Y_{\text{B}^{3+}} = 0.75$. The reaction expressing the

formation of NaBH₄ is given by (Eq. 49). Extending the NaH-NaBH₄ sub-binary composition line to the H₂-B elemental binary composition line renders the point of intersection where $Y_{B^{3+}} = 0.50$.



The elemental composition triangle's outer edges are comprised of two non-common-ion binary composition lines (i.e. Na⁺,B³⁺/Na⁻,B³⁻; B³⁺,H⁺/B³⁻,H⁻) and two common-ion, sub-binary composition lines (i.e. Na⁺/Na⁻,H⁻; Na⁺,H⁺/H⁻). The other four sub-binary composition lines that exist within the ternary composition space invoke the obvious ternary compound (NaBH₄) and are neither common-ion nor non-common-ion, and are herein defined as quasi-common-ion, sub-binary composition lines. In these cases, four ions exist; but, because of the formation of the ternary compound via the loss and gain of three ionic species at a definite ratio, along with the condition of charge neutrality (Eq. 18), as shown in the figure, an additional relationship allows for the sub-binary systems' compositions to be specified by one EEIF. Additionally, $Y_{B^{3+}}$ and Y_{Na^+} no longer span the range of zero to unity; rather, depending on the sub-binary composition line, their values either represent a maximum or minimum when the composition is NaBH₄.

The equivalent formation-reciprocal process given by (Eq. 50) is the analogue of the one given by (Eq. 40) in (2.2.3); it is graphically expressed by the stable pair line (Na-NaBH₄) which splits the NaH-Na-B-NaBH₄ composition domain into two distinct sub-ternary composition triangles (II and III). Cancellation of the supporting ion (H) and treatment of the elemental mixtures and compounds as salts renders (Eq. 51), which is simply the summation of the forward and reverse of (Eq. 33) and (Eq. 32), respectively.



Because there is only one anion, sub-ternary composition triangle I (H₂-NaH-NaBH₄) is additive (i.e. Na⁺,B³⁺,H⁺/H⁻) having the inequalities $Y_{B^{3+}}/Y_{Na^+} \leq 3$ and $Y_{B^{3+}}/Y_{H^-} \leq 0.75$; hence, specifying two cationic EEIFs defines composition. Graphically, compositions can be plotted using the EEIF coordinates $(Y_{Na^+}, Y_{H^+}, Y_{B^{3+}})$ on what is defined here as a partial Gibbs triangle. As one of the composition triangle's vertices is comprised of the obvious ternary compound, NaBH₄, a value of unity cannot be assigned to $Y_{B^{3+}}$; rather, the vertex is given by the coordinates (0.25,0,0.75). Furthermore, the forward and reverse of the amphoteric half-reaction given by (Eq. 22) suffices for the description of the possible electrochemical processes that can take place either within the sub-ternary region (i.e. mixing) or with respect to the other sub-ternary composition triangles in Fig. 13.

Along with $Y_{B^{3+}}/Y_{Na^+} \leq 3$, the Na-NaH-NaBH₄ ternary reciprocal composition half-square (i.e. II; B³⁺,Na⁺/Na⁻,H⁻) has for an inequality $Y_{Na^-}/Y_{Na^+} \leq 1$; it is the analogue of sub-ternary composition triangle II in Fig. 9 where, for electrochemical purposes, only the forward and reverse of the amphoteric half-reaction given by (Eq. 33) is required.

Both III and IV are defined as isothermal, isobaric, combinatorial, five-ion, equivalent, elemental, sub-ternary composition triangles. They differ from their analogues discussed hitherto (i.e. Fig. 7 and Fig. 8) in that no equivalence between the composition triangles' amphoteric species exists. However, along with the condition of charge neutrality (Eq. 18) we have a condition such that one cationic EEIF is a linear function of two anionic EEIFs and vice-versa. For III (i.e. B-Na-NaBH₄; Na⁺,B³⁺/Na⁻,B³⁻,H⁻) it is easily deduced that either $Y_{B^{3+}} = (3/4)Y_{H^-} + Y_{B^{3-}}$ or $Y_{Na^+} = (1/4)Y_{H^-} + Y_{Na^-}$ is true and therefore

composition can be plotted on a Gibbs (equilateral) triangle using the EEIF coordinates $(Y_{Na^-}, Y_{H^-}, Y_{B^{3-}})$. Similarly, for IV (i.e. B-H₂-NaBH₄; Na⁺, H⁺, B³⁺/B³⁻, H), it is found for ternary mixtures: $Y_{H^-} = 4Y_{Na^+} + Y_{H^+}$ or $Y_{B^{3-}} = 4Y_{B^{3+}} + 3Y_{H^+} - 3$ and that $Y_{Na^+} \leq 0.25$; hence, as was already discussed composition may be plotted on a partial Gibbs triangle using the EEIF coordinates $(Y_{Na^+}, Y_{H^+}, Y_{B^{3+}})$.

For III, the forward and reverse of the amphoteric half-reactions given by (Eq. 32) and (Eq. 33) are all that is required to describe the possible electrochemical processes, both within (mixing) and with respect to all of the other considered composition triangles. Similarly, for IV, amphoteric half-reactions (Eq. 32) and (Eq. 22) are sufficient. In regards to perfect galvanic cells, it is obviously nonsense to ponder solid ion electrolytes having transport numbers of unity for two distinct ionic species (i.e. Na⁺ and B³⁺); hence, only galvanic cells that employ solid ion electrolytes that are purely conductive towards H⁻ can be considered for the formation of NaBH₄. Furthermore, in order for the cell to approach its standard potential, the compositions of the cathode and anode compartments will approach that of pure H₂ and NaB, respectively.

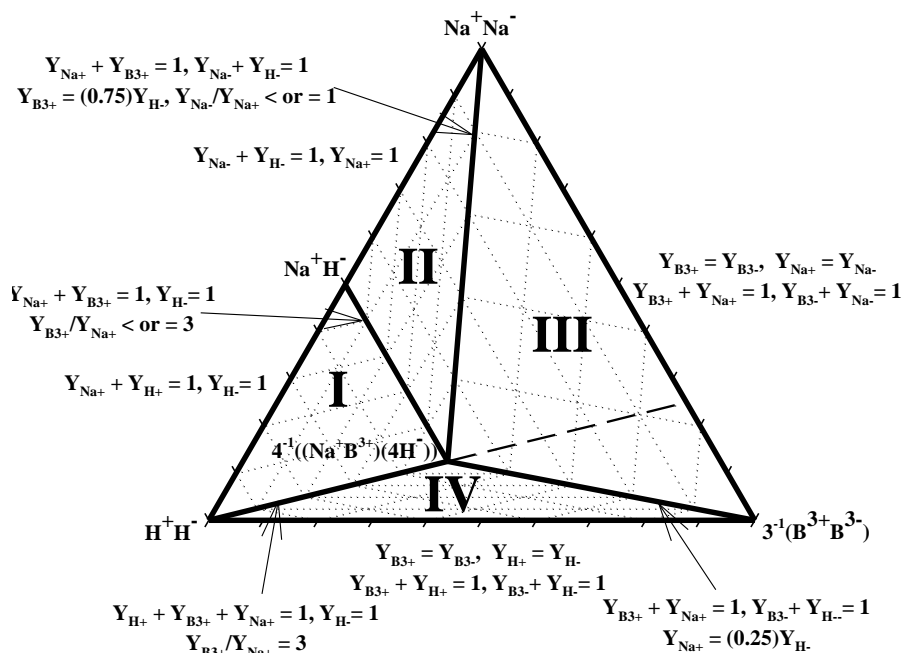


Fig. 13 Type-E, isothermal, isobaric, equivalent, elemental, ternary composition triangle for the B-Na-H system shown on the basis of EEIFs

Thus far four types of processes have been treated using the EEIF concentration scale and its corresponding electrochemical formalism (i.e. amphoteric half-reactions and MNE). They include: obvious compound formation (e.g. H-O), mixing (e.g. Na-B), reciprocal (e.g. hydrolysis), and reciprocal-formation (e.g. combustion).

2.3 The elemental Na-B-H-O quaternary system

The elemental Na-B-H-O quaternary composition space at or above ambient pressure and above and below the (thermal) decomposition temperatures of B₂H₆ and NaH, respectively, is represented by the composition regular tetrahedron in Fig. 14. Its outer surface is constructed out of two type-C (Na-B-O

and B-O-H), a type-D (Na-H-O), and a type-E (Na-B-H) elemental ternary composition triangles. The elemental quaternary space can be sub-divided into five stable sub-quaternary composition figures whereby a maximum of two of the four amphoteric half-reactions are possible in each when perfect electrochemical cells are considered.

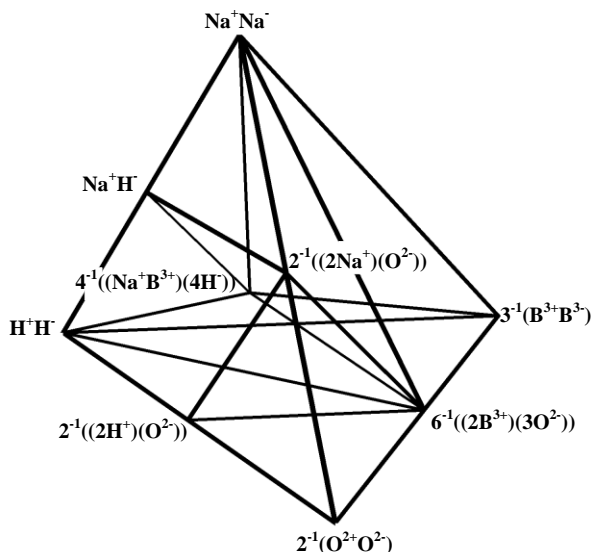


Fig. 14 Isothermal, isobaric, equivalent, elemental, quaternary composition regular tetrahedron for the Na-B-O-H system shown on the basis of EEIFs

Firstly, the transform of the $\text{Na}_2\text{O-B}_2\text{O}_3\text{-H}_2\text{O-O}_2$ sub-quaternary composition domain, shown in Fig. 15, belongs to the family of composition domains defined as an equivalent, elemental, additive, sub-quaternary composition regular tetrahedron (e.g. $\text{Na}^+, \text{B}^{3+}, \text{H}^+, \text{O}^{2+}/\text{O}^{2-}$); its sub-ternary analogue is the $\text{Na}_2\text{O-H}_2\text{O-O}_2$ system ($\text{Na}^+, \text{H}^+, \text{O}^{2+}/\text{O}^{2-}$; Fig. 10(b) (III)). All of the sub-quaternary composition domain's sub-binary composition lines comprising its outer edges have O^{2-} as their common-ion (i.e. $\text{Na}^+, \text{H}^+/\text{O}^{2-}$; $\text{B}^{3+}, \text{Na}^+/\text{O}^{2-}$; $\text{B}^{3+}, \text{H}^+/\text{O}^{2-}$; $\text{H}^+, \text{O}^{2+}/\text{O}^{2-}$; $\text{B}^{3+}, \text{O}^{2+}/\text{O}^{2-}$; and $\text{Na}^+, \text{O}^{2+}/\text{O}^{2-}$), and therefore its four outer faces are all additive ternary composition triangles (i.e. $\text{H}^+, \text{B}^{3+}, \text{Na}^+/\text{O}^{2-}$; $\text{Na}^+, \text{B}^{3+}, \text{O}^{2+}/\text{O}^{2-}$; $\text{H}^+, \text{Na}^+, \text{O}^{2+}/\text{O}^{2-}$; and $\text{H}^+, \text{B}^{3+}, \text{O}^{2+}/\text{O}^{2-}$). For simplicity's sake, the *less obvious compounds* (that are defined by their elements' ordering and not by their oxidation states) that exist within the $\text{Na}_2\text{O-B}_2\text{O}_3\text{-H}_2\text{O}$ ($\text{Na}^+, \text{B}^{3+}, \text{H}^+/\text{O}^{2-}$) sub-ternary composition triangle are not shown in the figure. From the condition of electroneutrality (Eq. 18), three compositional variables can be represented by the composition regular tetrahedron. Any arbitrary point within the three-dimensional composition space will have its components' concentrations determined by extending four lines from the point to the planes opposite the four components given that the lines run parallel to one of the three edges that commence at the pure component (i.e. the tetrahedron's vertices) [49]. Without proof, it is known that the summation of the lines lengths is equal to the length of any of the composition space's outer edges (i.e. unity). Since these sub-quaternary mixtures contain only one amphoteric species (i.e. O_2), if perfect electrochemical cells are conceived with anolyte and catholyte compositions belonging to the composition space, only the amphoteric half-reaction given by either the forward or reverse of (Eq. 23) is required. As well, given that three compositional variables are known, if an electrochemical cell's anolyte or catholyte is made up of a mixture belonging to the sub-quaternary

composition space, then either the forward or the reverse of (Eq. 23) will sufficiently describe the half-reaction taking place in the relevant compartment.

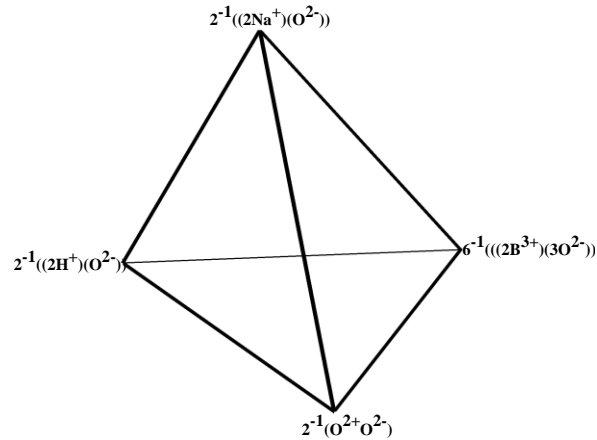


Fig. 15 Isothermal, isobaric, equivalent, elemental, additive, sub-quaternary composition regular tetrahedron for the $\text{Na}_2\text{O}-\text{B}_2\text{O}_3-\text{H}_2\text{O}-\text{O}_2$ ($\text{Na}^+, \text{B}^{3+}, \text{H}^+, \text{O}^{2+}/\text{O}^{2-}$) system shown on the basis of EEIFs

Secondly, under isothermal and isobaric conditions, the composition space transforms into the herein defined equivalent, elemental, reciprocal, sub-quaternary composition quasi-triangular-prism ($\text{Na}^+, \text{B}^{3+}, \text{H}^+/\text{H}^-, \text{O}^{2-}$; Fig. 16). More generally, these three-dimensional composition domains are either three-cation, two-anions or two-cation, three anion mixtures whereby the mixtures only amphoteric species is positioned at one of the vertices. The pentahedron's outer surfaces include three two-anion, two-cation composition squares and two one-anion, three-cation or three-anion, one-cation additive composition triangles (the basal faces). In this particular case, these surfaces correspond to the $\text{Na}^+, \text{B}^{3+}/\text{O}^{2-}, \text{H}^+$, $\text{Na}^+, \text{H}^+/\text{H}^-, \text{O}^{2-}$, and $\text{B}^{3+}, \text{H}^+/\text{H}^-, \text{O}^{2-}$, reciprocal sub-ternary composition squares, and the $\text{B}^{3+}, \text{Na}^+, \text{H}^+/\text{H}^-$, and $\text{Na}^+, \text{B}^{3+}, \text{H}^+/\text{O}^{2-}$ additive sub-ternary composition triangles. The author previously investigated the liquidus topology [34] of the most former system and some of its less obvious compounds are indicated in the diagram for the purposes of this discussion. The triangulations that result from the reciprocal reactions (i.e. (Eq. 2), (Eq. 6), and (Eq. 7)) subdivide the composition space into stable hydrous ($\text{Na}_2\text{O}-\text{B}_2\text{O}_3-\text{H}_2\text{O}-\text{H}_2$; tetrahedron) and anhydrous ($\text{Na}_2\text{O}-\text{B}_2\text{O}_3-\text{NaBH}_4-\text{NaH}-\text{H}_2$; quasi-base pyramid) regions.

All of the possible electrochemical processes within the triangular prism are expressible by the combination of the forward or reverse of (Eq. 22). As is the case for its ternary analogue (2.2.4), galvanic cells comprised of hydrous (cathode) and anhydrous (anode) mixtures will theoretically produce H_2 at both electrodes due to the simultaneous electro-reduction and electro-oxidation of H^+ (H_2O) and H^- (e.g. NaBH_4), respectively.

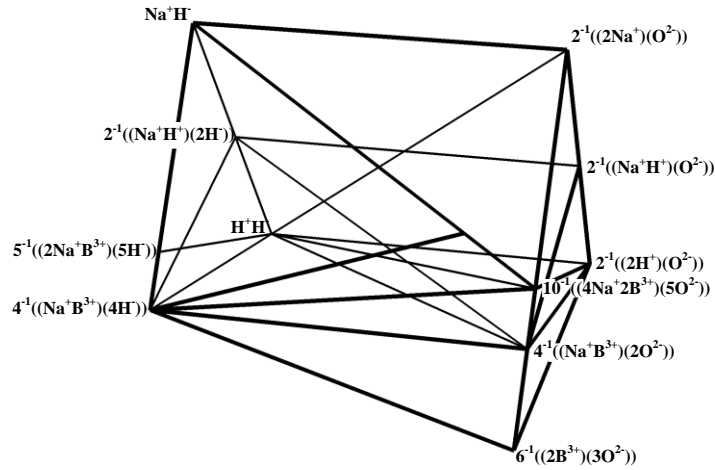
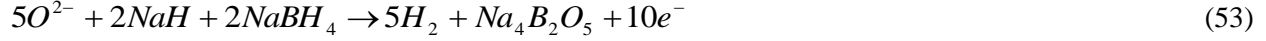


Fig. 16 Isothermal, isobaric, equivalent, elemental, quasi-reciprocal, sub-quaternary composition quasi-triangular-prism for the $\text{NaH-Na}_2\text{O-B}_2\text{O}_3\text{-NaBH}_4\text{-H}_2\text{O-H}_2$ ($\text{Na}^+, \text{B}^{3+}, \text{H}^+/\text{H}^-, \text{O}^{2-}$) system shown on the basis of EEIFs

The $\text{H}_2\text{-NaBH}_4$ binary composition line has for conditions: $Y_{\text{H}^-} = 1$, $Y_{\text{Na}^+} + Y_{\text{B}^{3+}} + Y_{\text{H}^+} = 1$, and $Y_{\text{Na}^+}/Y_{\text{B}^{3+}} = 1/3$. By inserting the constant ratio into the summation cationic EEIFs we have $(4/3)Y_{\text{B}^{3+}} + Y_{\text{H}^+} = 1$; hence, like regular common-ion binary composition lines, the specification of one EEIF suffices to define composition. For the $\text{NaBH}_4\text{-B}_2\text{O}_3$ quasi-common-ion sub-binary composition line $Y_{\text{Na}^+} + Y_{\text{B}^{3+}} = 1$, $Y_{\text{H}^-} + Y_{\text{O}^{2-}} = 1$, and $Y_{\text{Na}^+} = (4)^{-1}Y_{\text{H}^-}$. By substitution we have $Y_{\text{B}^{3+}} = 1 - (4)^{-1}Y_{\text{H}^-}$, and therefore a single anionic or cationic EEIF specifies composition. Assigning composition coordinates to the triangular prism is done by assigning one of the additive ternary composition (Gibbs) triangles the coordinates $(Y_{\text{H}^+}, Y_{\text{Na}^+}, Y_{\text{B}^{3+}})$ while assigning either Y_{H^-} or $Y_{\text{O}^{2-}}$ to the vertical axis.

Several equivalent, elemental, quasi-reciprocal ternary composition squares are shown within the composition quasi-triangular-prism. Triangulations of said composition squares illustrates the processes given by (Eq. 2), (Eq. 5), (Eq. 6), and (Eq. 7). Hypothetical galvanic and electrolytic cells of the design given schematically in Table 2 and Fig. 2 utilizing SOAEs may be conceivable to test simple ERH (or ERC) processes. It was previously found that NaBO_2 is at best only sparingly soluble in liquid NaBH_4 , and therefore simple ERH processes, as they relate to $\text{Na}_4\text{B}_2\text{O}_5$, should be considered. The $5^{-1}\text{Na}_2\text{BH}_5\text{-}10^{-1}\text{Na}_4\text{B}_2\text{O}_5\text{-}2^{-1}\text{H}_2\text{O-H}_2$ equivalent, elemental, reciprocal, quasi-ternary composition square can be found in the three-dimensional composition domain; it allows one to express the desirable hydrolysis (Eq. 7) and ERH (Fig. 2) processes that were discussed in (1.2). The standard galvanic cell's anolyte and catholyte compositions would approach those of pure Na_2BH_5 and H_2O , respectively. The half-reactions, as they would be assigned in standard electrochemical textbooks, are given by (Eq. 52) and (Eq. 53); but with the cancellation of the unaffected ions (Na^+ , B^{3+} and O^{2-}), the reactions simplify to the forward and reverse of the amphoteric half-reaction given by (Eq. 22). Sketches of galvanic hydrolysis and combustion (reciprocal-formation) cells would closely mimic those given by (Fig. 11) and (Fig. 12) in (2.2.4); their electrolytic analogues are ponderable assuming that the cell's polarity is reversed and a significant

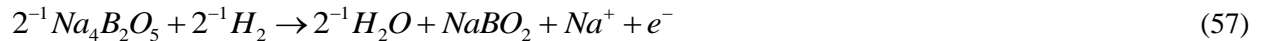
amount of $\text{Na}_4\text{B}_2\text{O}_5$ is present in the catholyte. As was previously pointed out [34], given the liquidus topology of the $\text{Na}_2\text{BH}_5\text{-Na}_4\text{B}_2\text{O}_5$ quasi-binary system, state-of-the-art SOAE technology is sufficient to test either ERH or ERC.



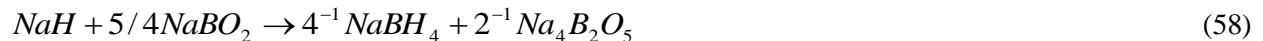
Considerations of the electrochemical energy transformation for the process given by (Eq. 5) is facilitated by the composition square (taken from the pentahedron) having 4^{-1}NaBH_4 , 4^{-1}NaBO_2 , 2^{-1}NaOH , and $2^{-1}(\text{NaH-H}_2)$ as its corners. If the standard potential of the reaction is to be measured, the catholyte and anolyte mixtures would be constituted by nearly pure NaOH and NaBH₄, respectively. Conventionally, the respective half-reactions could be given by (Eq. 54) and (Eq. 55). Evidently, the electrochemical cell would require a SOAE as only the O^{2-} anion could carry the internal current. Again, by treating the compounds as completely ionic, cancelling out the supporting ions (i.e. Na^+ , B^{3+} , and O^{2-}), and dividing both half-reactions by the number of electrons, such that it is given on an equivalent basis, the electro-reduction and electro-oxidation reactions are equivalent to the forward and reverse of (Eq. 22). Furthermore, if the half-reactions are written on an equivalent basis, their summation results in the process given by (Eq. 5), and using this stoichiometry and standard thermodynamic literature values for the compounds, it is possible to estimate the standard potential for this hypothetical galvanic cell and therefore the minimum potential required to reverse the reaction via an electrolytic cell. As the forward and reverse of (Eq. 22) is responsible for the measured potential, the MNE is expressed as it was previously (Eq. 44); the notation must be modified slightly by substituting ${}^{\text{Na}^+, \text{B}^{3+}, \text{H}^+ / \text{H}^-, \text{O}^{2-}} \Delta E$ to account for the higher order system.



The quaternary ERH and ERC processes considered thus far have been simple as theoretically oxides are directly regenerated to hydrides and there is no need for an additional solvent extraction circuit. However, the previous assertion [34] that only SOAE would suffice for the electrolytic regeneration of NaBH₄ from its respective oxide was too rash. Other, more complex, ERH processes that employ solid alkaline metal cation electrolytes could be considered. For example, an ERH process whereby the cathode and anode compartments are comprised of mixtures of $\text{H}_2\text{-NaBO}_2\text{-Na}_4\text{B}_2\text{O}_5\text{-H}_2\text{O}$ and $\text{H}_2\text{-NaH-NaBH}_4$, respectively, and a SSCE ($\beta''\text{-Al}_2\text{O}_3$) seems plausible. The theoretical half-reactions at the respective electrodes are given by (Eq. 56) and (Eq. 57). Again, upon cancellation of the unaffected ions on both sides of each half reaction renders the forward and reverse of (Eq. 22).



Following the dehydration of the molten salt hydrate, $\text{NaBO}_2 \cdot x\text{H}_2\text{O}$, NaBH₄ may be produced via the previously-discovered [34], quasi-reciprocal reaction (Eq. 58). The block diagram given in Fig. 17 indicates that the combined processes equates to the reverse of (Eq. 2).



For mass transfer to the anolyte/anode interface to be maintained, the molten salt hydrate $\text{Na}_4\text{B}_2\text{O}_5 \cdot x\text{H}_2\text{O}$ has been suggested for the hypothetical ERH unit operation's anodic feedstock. For the same reason, liquid NaBH₄ is recycled into the ERH cathode compartment. In addition, the polar organic solvent extraction circuit is included for the separation of the $\text{Na}_4\text{B}_2\text{O}_5$ from NaBH₄. Because of the

hazard that would result from any unintended anolyte-catholyte mixing in the ERH unit operation, along with the increased complexity of this process compared to the one given in Fig. 3, complex ERH/ERCO processes are less desirable than the simpler sort where a H_2 - H_2O gas/vapour mixture comprises the ERH unit operation's anolyte.

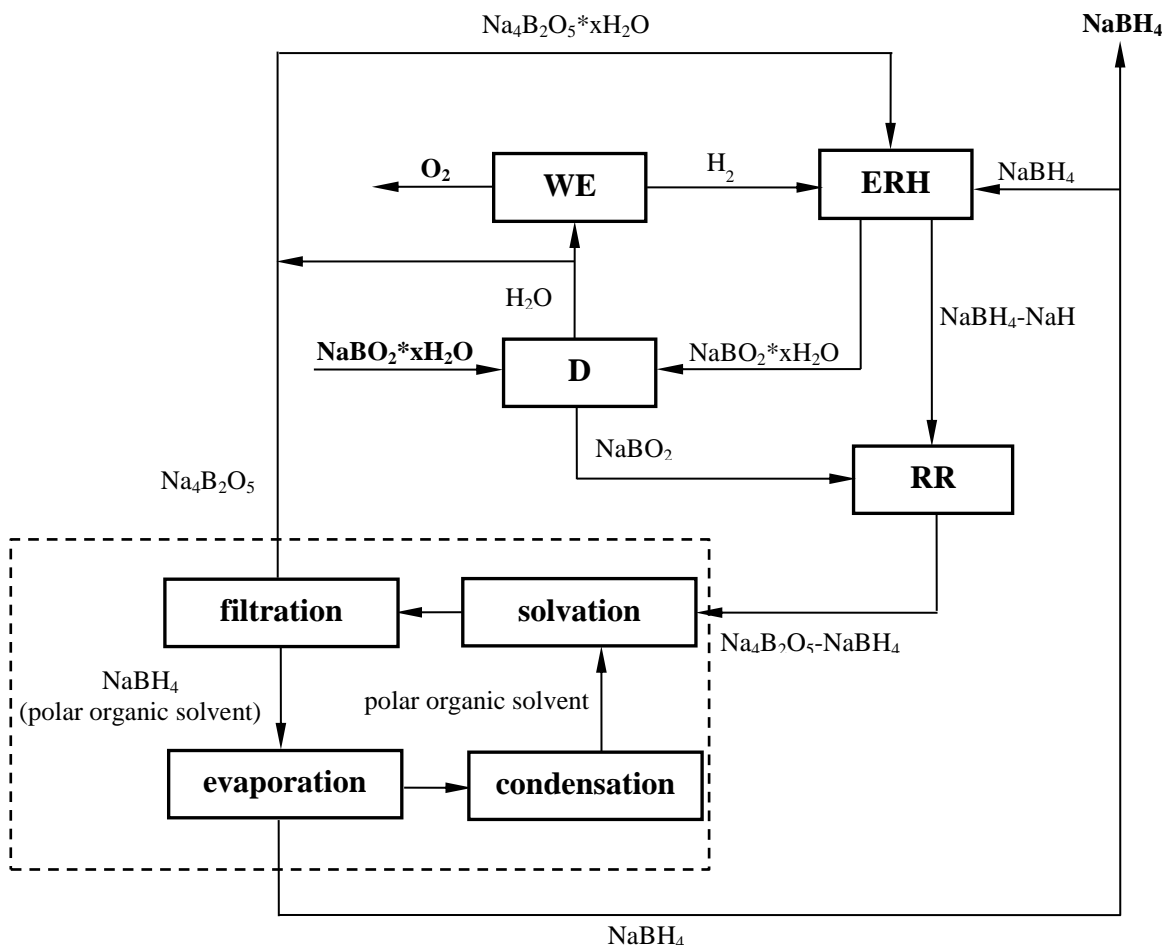


Fig. 17 Block diagram for hypothetical, steady-state, complex ERCO process (~ 1.0 MPa; ~ 823 °K) that utilizes SSCE technology in the ERH unit operation and a solvent extraction circuit for the separation of $NaBH_4$ from $Na_4B_2O_5$ – D - dehydration; WE - water electrolysis; RR - quasi-reciprocal reaction (Eq. 58)

Shown in Fig. 18 is the B - B_2O_3 - $NaBH_4$ - Na ($Na^+, B^{3+}/B^{3-}, Na^-, H, O^{2-}$) isothermal, isobaric, elemental, equivalent, combinatorial sub-quaternary composition tetrahedron. Conditions pertaining to its common-ion (i.e. $B^{3+}/B^{3-}, O^{2-}$) non-common-ion (i.e. $B^{3+}, Na^+/Na^-, O^{2-}$), and quasi-common-ion (i.e. $B^{3+}, Na^+/Na^-, H$; $Na^+, B^{3+}/Na^-, B^{3-}$; $B^{3+}, Na^+/O^{2-}, H$; $B^{3+}, Na^+/O^{2-}, H$) sub-binary composition lines are given in the figure, and discussions regarding the B - $NaBH_4$ - Na and Na - B_2O_3 - B ternary composition triangles are given in sections 2.2.5 and 2.2.3, respectively.

The composition tetrahedron's outer faces $NaBH_4$ - B - B_2O_3 ($B^{3+}, Na^+/B^{3-}, O^{2-}, H$) and Na - B_2O_3 - $NaBH_4$ ($B^{3+}, Na^+/Na^-, O^{2-}, H$) are further examples of isothermal, isobaric, combinatorial, five-ion,

*Corresponding author Tel.: +1 819 821 8000ext63238; fax: +1 819 821 7095

E-mail: danielcalabretta@gmail.com

equivalent, elemental, sub-ternary composition triangles (2.2.5). In regards to ternary mixtures, the former's are bound by the condition $Y_{H^-} = 4Y_{Na^+}$ (or $Y_{O^{2-}} + Y_{B^{3-}} + 3 = 4Y_{B^{3+}}$) and the latter's are constrained by $Y_{Na^+} = (1/4)Y_{H^-} + Y_{Na^-}$ (or $Y_{B^{3+}} = (3/4)Y_{H^-} + Y_{O^{2-}}$). Both may be graphically plotted on Gibbs (equilateral) triangles by employing their respective three anionic EEIFs (i.e. $(Y_{B^{3-}}, Y_{O^{2-}}, Y_{H^-})$ and $(Y_{Na^-}, Y_{O^{2-}}, Y_{H^-})$) as coordinates.

Along with the condition of electroneutrality (Eq. 18) the additional relationship $Y_{Na^+} = 4^{-1}Y_{H^-} + Y_{Na^-}$ (or $Y_{B^{3+}} = (3/4)Y_{H^-} + Y_{O^{2-}} + Y_{B^{3-}}$) makes it so that, as is the case when using mass or mole fractions, a quaternary mixture's composition is defined if three anionic EEIFs are specified; furthermore, like its additive sub-quaternary analogue (Fig. 18), the four anionic EEIF coordinates are sufficient for the geometrical presentation of composition. Because quaternary mixtures contains two amphoteric species (i.e. boron and sodium), all of the possible electrochemical processes within the composition domain (i.e. mixing) may be expressed by either the forward or reverse of either (Eq. 32) or (Eq. 33). Electrochemical processes implicating the other sub-quaternary mixtures belonging to the Na-B-O-H system will include either the forward or reverse of the same amphoteric half-reactions or mixtures thereof (e.g. the formation of $NaBH_4$; 2.2.5) in the electrochemical cell's compartment containing the stable quaternary mixture.

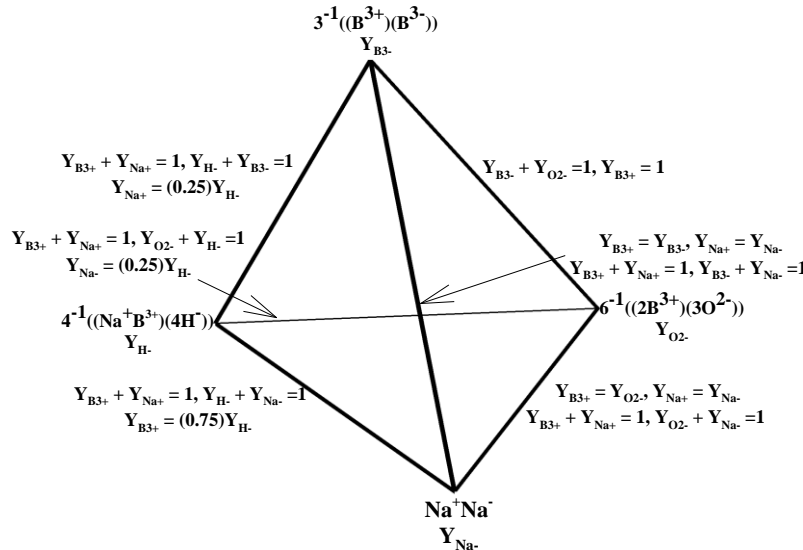


Fig. 18 Isothermal, isobaric, elemental, equivalent, combinatorial, additive, sub-quaternary composition regular tetrahedron for the $B-B_2O_3-NaBH_4-Na$ ($Na^+, B^{3+}/B^{3-}, Na^-, H, O^{2-}$) composition domain shown on the basis of EEIFs

In Fig. 19 an isothermal, isobaric, elemental, equivalent sub-quaternary composition oblique irregular-base-pyramid represents mixtures of the $NaBH_4-Na-NaH-B_2O_3-Na_2O$ ($B^{3+}, Na^+/Na^-, H, O^{2-}$) composition domain. Conditions pertaining to its eight sub-binary composition lines (edges) are given in the figure. Five ternary composition figures enclose the sub-quaternary region: The $NaH-Na_2O-NaBH_4-B_2O_3$ ($Na^+, B^{3+}/H, O^{2-}$) quasi-reciprocal ternary composition square constitutes the figure's base and interfaces with the sub-quaternary quasi-reciprocal composition quasi-triangular-prism (Fig. 16), while two right-angled composition

half-squares (i.e. $B^{3+}, Na^+/Na^-, H^-$ and $B^{3+}, Na^+/Na^-, O^{2-}$) in which the inequality $Y_{Na^-}/Y_{Na^+} \leq 1$ holds, constitute the sub-quaternary system's sides. For the Na-NaBH₄-B₂O₃ ($B^{3+}, Na^+/Na^-, H^-, O^{2-}$) five-ion, combinatorial ternary composition triangle, because of the condition $Y_{B^{3+}} = (3/4)Y_{H^-} + Y_{O^{2-}}$, mixtures thereof can be graphically represented on a Gibbs (equilateral) triangle having coordinates $(Y_{Na^-}, Y_{H^-}, Y_{O^{2-}})$. Finally the Na₂O-NaH-Na ($Na^+/Na^-, H^-, O^{2-}$) sub-ternary additive composition triangle (Fig. 10(b); I) is orthogonal to the quasi-reciprocal ternary composition square.

Compositions of sub-quaternary mixtures are uniquely defined by any one of the four three-EEIF permutations: $(Y_{Na^-}, Y_{Na^+}, Y_{O^{2-}})$, $(Y_{Na^-}, Y_{B^{3+}}, Y_{O^{2-}})$, $(Y_{Na^-}, Y_{Na^+}, Y_{H^-})$, or $(Y_{Na^-}, Y_{B^{3+}}, Y_{H^-})$. The assignment of EEIF coordinates for this composition figure is beyond the scope of this article. For any sub-quaternary mixture the condition $Y_{Na^-}/Y_{Na^+} \leq 1$ exists and the forward or reverse of the amphoteric half-reaction given by (Eq.33) sufficiently describes all of the possible electrochemical processes both within the sub-quaternary region (mixing) and with respect to all other sub-quaternary mixtures contained within the Na-B-O-H composition domain.

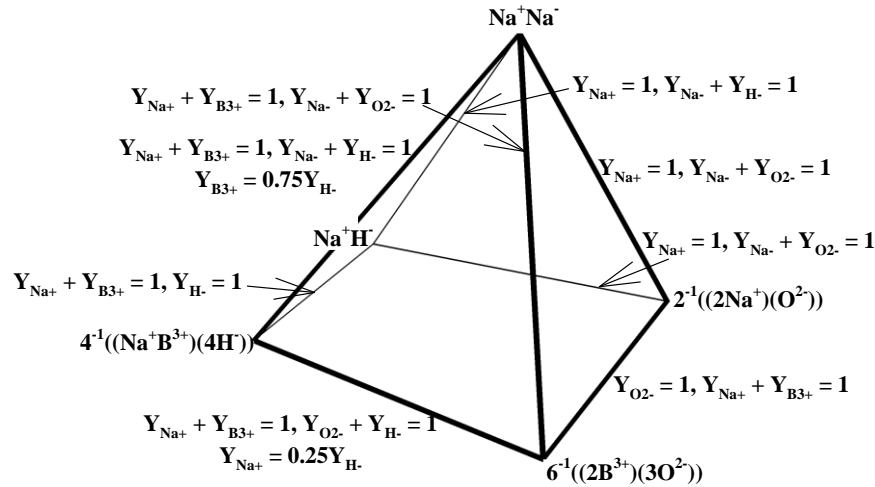


Fig. 19 Isothermal, isobaric, equivalent, combinatorial, sub-quaternary composition oblique, irregular base pyramid for the NaBH₄-Na-NaH-B₂O₃-Na₂O ($B^{3+}, Na^+/Na^-, H^-, O^{2-}$) composition domain shown on the basis of EEIFs

Fig. 20 shows the isobaric, isothermal, three-cation, three-anion, combinatorial, sub-quaternary composition regular tetrahedron H₂-NaBH₄-B-B₂O₃ ($Na^+, B^{3+}, H^+/H^-, B^{3-}, O^{2-}$). Of its six outer edge sub-binary composition lines one is common-ion ($B^{3+}/B^{3-}, O^{2-}$), two are non-common-ion ($H^+, B^{3+}/B^{3-}, H^-; B^{3+}, H^+/H^-, O^{2-}$), and three are quasi-common-ion. The quasi-common-ion composition lines include NaBH₄-B ($Na^+, B^{3+}/B^{3-}, H^-$), NaBH₄-B₂O₃ ($Na^+, B^{3+}/H^-, O^{2-}$) and NaBH₄-H₂ ($Na^+, B^{3+}, H^+/H^-$) the conditions for which are given in the figure. Discussions pertaining to the sub-ternary composition triangles NaBH₄-B-H₂ ($Na^+, B^{3+}, H^+/H^-, B^{3-}$), NaBH₄-B₂O₃-H₂ ($Na^+, B^{3+}, H^+/H^-, O^{2-}$), and NaBH₄-B₂O₃-B ($Na^+, B^{3+}/B^{3-}, H^-, O^{2-}$) are given in relation to Fig. 13, Fig. 16, and Fig. 18, respectively, and the relation $Y_{H^+} = Y_{H^-}$ holds true for the H₂-B-B₂O₃ ($H^+, B^{3+}/B^{3-}, H^-, O^{2-}$) five-ion, ternary composition triangle. For sub-quaternary mixtures, the relationship $4Y_{Na^+} + Y_{H^+} + Y_{O^{2-}} + Y_{B^{3-}} = 1$ and the inequalities $Y_{Na^+} \leq 1/4$ and $Y_{Na^+}/Y_{B^{3-}} \leq 1/3$ are easily deduced; hence, their graphical presentation is made possible by utilizing a composition regular tetrahedron having the EEIF coordinates $(4Y_{Na^+}, Y_{H^+}, Y_{O^{2-}}, Y_{B^{3-}})$.

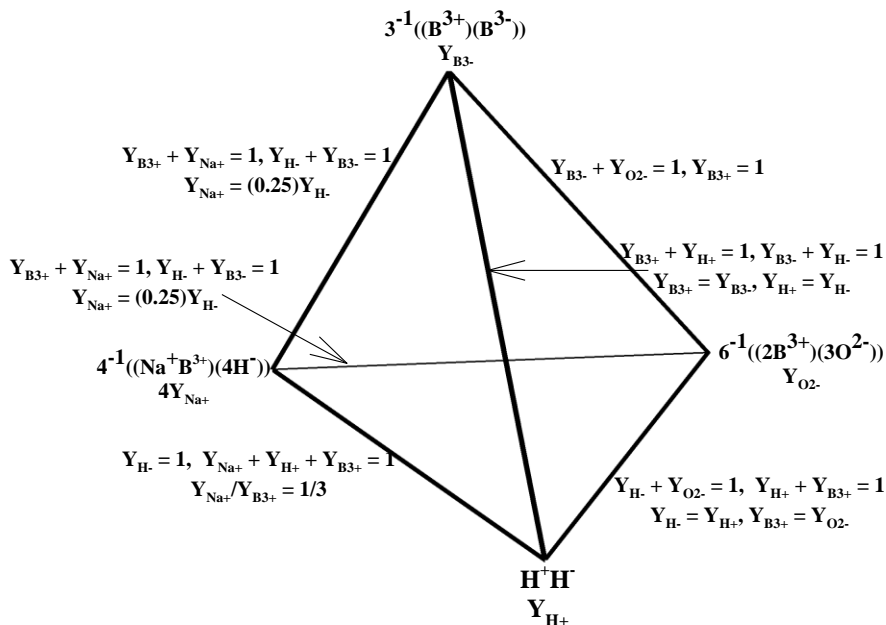


Fig. 20 Isothermal, isobaric, equivalent, combinatorial, sub-quaternary composition irregular tetrahedron for the B-H₂-NaBH₄-B₂O₃ (Na⁺, B³⁺, H⁺/H⁻, B³⁻, O²⁻) composition domain shown on the basis of EEIFs

Conclusions

On a volumetric energy density basis, solid light-alkaline-metal-borohydride complete oxidation processes are the most analogous to those used for vehicular propulsion. During said processes, carbon or boron and its accompanying light-alkaline-metal retain their positive formal charge as hydrogen's formal charge undergoes a change from negative to positive and O₂ loses all of its positive character so that the oxygen holds a purely negative formal charge in the produced compounds. As well, both steam hydrocarbon reformation and metal hydride hydrolysis processes may be regarded as metathesis reactions and therefore H₂ may be treated as a salt. As H₂ is a gas at ambient conditions and a low-density liquid at cryogenic temperatures, and because only one of its constituents can possess a negative formal charge, it cannot be considered as an evolutionary automotive fuel.

As the electrochemical series incorporates a notional concentration scale that seemingly cannot account for electrochemical cells comprised of anolytes and catholytes of vastly different character, and due to the redundancy in adding different sets of redox reactions for the expression of what are essentially the same processes, an alternate view of the electrochemical series has been put forth in a so-called amphoteric formalism which, at its core, employs a new concentration scale akin to equivalent ionic fractions. The formalism allows one to predict which solid ion electrolytes are permissible for a particular electrochemical process; furthermore, it allows for an equivalent graphical presentation of elemental composition domains that can be divided into regions of stability so that a minimum number of half-reactions need be considered, and so that the independent anolyte and catholyte mixtures may be defined by the ratio of their respective amphoteric element's EEIFs. Three types of equivalent, elemental, binary and sub-binary composition lines facilitated the construction of five types of elemental, equivalent, ternary composition triangles, which in turn facilitated the construction of the equivalent, elemental, Na-B-H-O quaternary composition tetrahedron. These isothermal, isobaric, composition figures aid in the

*Corresponding author Tel.: +1 819 821 8000ext63238; fax: +1 819 821 7095

E-mail: danielcalabretta@gmail.com

illustration of numerous electrochemical processes including: mixing, obvious compound formation, reciprocal, and reciprocal-formation. Moreover, the formalism allows for a more lucid description of the types of electrolysis cells that will be required to achieve the desired ERCO processes, which, in the author's view, are essential for the future of mobile power systems. Over time the generalization of this formalism will be determined.

Of course, the discussions of hypothetical cells like those given in Table 2, Fig. 2, Fig. 11, and Fig. 12 have been oversimplified; for, it is essential to understand the interaction(s) between the anolyte and catholyte with their respective electrodes and the solid ion electrolyte(s). An initial study that implicates the amphoteric formalism is available [50].

Acknowledgements

The author would like to express his gratitude towards Kingston Process Metallurgy Inc., AUTO21, and NSERC for financing this work.

References

- [1] http://www1.eere.energy.gov/hydrogenandfuelcells/storage/pdfs/targets_onboard_hydro_storage_explanation.pdf
- [2] http://www.nap.edu/catalog.php?record_id=11406
- [3] http://www.hydrogen.energy.gov/pdfs/review04/st_1_miliken.pdf
- [4] http://www.hydrogen.energy.gov/pdfs/progress09/i_introduction.pdf
- [5] Pelton AD, Schmalzried H (1973) *Met. Trans.* 4: 1395-1404
- [6] Leung WB, March NH, Motz H (1976) *Physics Letters A* 56(6): 425-426
- [7] <http://www1.eere.energy.gov/hydrogenandfuelcells/pdfs/32405b2.pdf>
- [8] <http://www.nrel.gov/docs/fy03osti/32525.pdf>
- [9] Zuttel A (2003) *Mater. Today* 6(9): 24-33
- [10] http://www.hydrogen.energy.gov/pdfs/review10/st003_berry_2010_o_web.pdf
- [11] http://www1.eere.energy.gov/hydrogenandfuelcells/pdfs/best_practices_hydrogen_storage.pdf
- [12] Wojciech G, Edwards P (2004) *Chemical Reviews* 104: 1283-1315
- [13] Orimo S, Nakamori Y, Eliseo JR, Zuttel A, Jensen CM (2007) *Chemical Reviews* 107: 4111-4132
- [14] http://www.hydrogen.energy.gov/pdfs/progress09/iv_b_1a_ott.pdf
- [15] http://www.hydrogen.energy.gov/pdfs/progress08/iv_b_1g_sneddon.pdf
- [16] Retnamma R, Novais AQ, Rangel CM (2011) *Int. J. Hydrogen Energy* 36(16): 9772-9790
- [17] <http://www.hydrogen.energy.gov/pdfs/42220.pdf>
- [18] http://www.hydrogen.energy.gov/pdfs/progress07/iv_b_5a_moreno.pdf
- [19] http://www.hydrogen.energy.gov/pdfs/progress06/iv_b_4d_wu.pdf
- [20] http://www.hydrogen.energy.gov/pdfs/progress04/iiib1_wu.pdf
- [21] http://www.hydrogen.energy.gov/pdfs/progress06/iv_b_1_wu.pdf
- [22] http://www.hydrogen.energy.gov/pdfs/progress06/iv_b_4c_linehan.pdf
- [23] http://www.hydrogen.energy.gov/pdfs/progress07/iv_b_5b_linehan.pdf
- [24] http://www.hydrogen.energy.gov/pdfs/progress06/iv_b_4e_macdonald.pdf
- [25] http://www.hydrogen.energy.gov/pdfs/progress07/iv_b_5c_macdonald.pdf
- [26] Celik C, San FGB, Sarac HI (2010) *J. Power Sources* 195(9): 2599-2603
- [27] Ma J, Choudhury NA, Sahai Y (2010) *Renewable and Sustainable Energy Reviews* 14(1): 183-199
- [28] Saboungi M, Blander M (1974) *J. Am. Chem. Soc.* 58(1-2): 1-7
- [29] Prosini PP, Gislou P (2010) *Int. J. Hydrogen Energy* 35(22) 12234-12238
- [30] Ferreira MJF, Gales L, Fernandes VR, Rangel CM, Pinto AMFR (2010) *Int. J. Hydrogen Energy* 35(18): 9869-9878
- [31] Oronzio R, Monteleone G, Pozio A, De Francesco M, Galli S (2009) *Int. J. Hydrogen Energy* 34(10): 4555-4560
- [32] Shafirovich E, Diakov V, Varma A (2007) *Int. J. Hydrogen Energy* 32(2): 207-211
- [33] Gislou P, Monteleone G, Prosini PP (2009) *Int. J. Hydrogen Energy* 34(2): 929-937
- [34] Calabretta DL, Davis BR (2007) *J. Power Sources* 164(2): 782-791
- [35] Kuznetsov VA, Mikheeva VI (1970) *Russ. J. Inorg. Chem.* 15(6): 849-850

*Corresponding author Tel.: +1 819 821 8000ext63238; fax: +1 819 821 7095

E-mail: danielcalabretta@gmail.com

- [36] Calabretta DL (2006) Master's thesis, Queen's University
- [37] Vajo JJ, Liu P (2010) US Patent 7,776,201
- [38] Calabretta DL (2009), Proceedings of the 2009 Hydrogen and Fuel Cells Conference, Vancouver, Canada.
- [39] Laity R, in Ives D and Janz D, eds., Reference Electrodes, Academic Press, New York, 1961, Chap. 12
- [40] Blander M, in M. Blander, eds, Molten Salt Chemistry, John Wiley and Sons, New York, 1964, Chap. 2
- [41] Pelton AD, Chartrand P (2001) Met. Mater. Trans. A 32A(6): 1355-1360
- [42] Gibbs JW, The scientific papers of J. Willard Gibbs, Longmans Green and co., London New York and Bombay, 1906, pg 425
- [43] Guggenheim A (1928) J. Phys. Chem. (33): 842-849
- [44] Pauling L; The Nature of the Chemical Bond and the Structure of Molecules and Crystals (3rd Edition), Cornell University Press, Ithaca New York, 1960, pg. 27
- [45] Buck RP, Rondinini S, Covington AK, Baucke FGK, Brett CMA, Camões MF, Milton MJT, Mussini T, Naumann R, Pratt KW, Spitzer P, Wilson GS (2002) J. Appl. Chem. 74(11): 2169-2200
- [46] Blander M, Yosim SJ (1963) J. Chem. Phys. 39: 2610-2617
- [47] Shunk FA, Hansen M, Constitution of binary alloys: Second supplement, McGraw-Hill, New York, Toronto, 1969 pg. 92
- [48] Bridges CA, Fernandez-Alonso F, Goff JP, Rosseinsky MJ (2006) Advanced Mater.18: 3304-3308
- [49] Zhao JC ed, Methods for Phase Diagram Determination, Elsevier, Oxford, 2007
- [50] <http://www.scribd.com/doc/125222178/On-the-Compatibility-of-Electronic-Insulators-and-Ionic-Conductors-With-the-Na2BH5-Na4B2O5-H2-Quasi-ternary-System>
- [51] Patnaik P, Handbook of Inorganic Chemicals, McGraw-Hill, New York, 2003
- [52] König Von H, Hoppe R, Jansen M (1979) Z. Anorg. Allg. Chem. 449: 91-101
- [53] Guggenheim EA, Thermodynamics: an advanced treatment for chemists and physicists 5th ed., North-Holland Publishing Co., Amsterdam, 1967, pp 268, 302